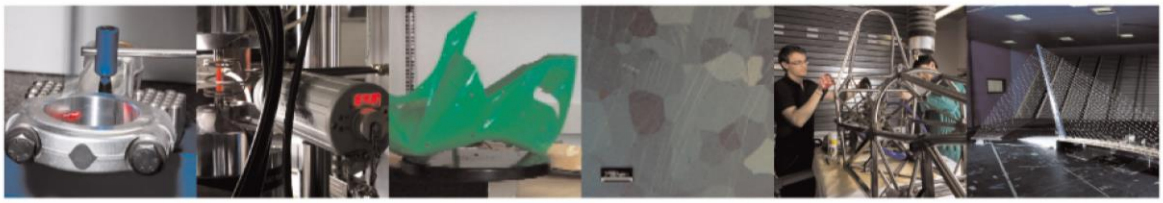

# A cost model for the economic evaluation of in-situ monitoring tools in metal additive manufacturing

Colosimo, B. M.; Cavalli, S.; Grasso, M.

This is a post-peer-review, pre-copyedit version of an article published in INTERNATIONAL JOURNAL OF PRODUCTION ECONOMICS. The final authenticated version is available online at: http://dx.doi.org/10.1016/j.ijpe.2019.107532



DIPARTIMENTO DI MECCANICA ■ POLITECNICO DI MILANO
via G. La Masa, 1 ■ 20156 Milano ■ EMAIL (PEC): pecmecc@cert.polimi.it
http://www.mecc.polimi.it
Rev. 0

# A Cost Model for the Economic Evaluation of In-situ Monitoring Tools in Metal Additive Manufacturing

*Abstract*

The paper presents a cost model to evaluate the economic impact of defects and process instability in metal Additive Manufacturing (AM). The proposed model formulation adopts the main framework of previous seminal studies and extends it by considering the contribution of scrap fractions and in-situ monitoring performances on process and material costs, including pre- and post-processing operations. Three real industrial case studies (from dental, aerospace, and machinery sectors) were assessed to determine how the model can be used in the real industrial practice to (i) enhance the economic advantages of metal AM technologies by tackling process instability issues, (ii) assess the effectiveness of in-situ monitoring in the development of next generation metal AM systems, and (iii) define the performance specifications of in-situ monitoring solutions that yield sustainable cost savings in specific industrial applications. A further experimentation is presented to validate the cost model with respect to a benchmark reference.

**Keywords**: laser powder bed fusion; cost modelling; economic analysis; in-situ monitoring

## 1. INTRODUCTION

The metal additive manufacturing (AM) market has been growing at double-digit rates in the past few years due to continuous technological developments and strategic programs that foster public and private investments in this field. The increasing interest for AM implementation in industry is characterized by a significant shift from earlier prototyping applications to a wide range of possible applications of metal AM for the manufacturing of functional products. This growth was enabled by several advantages of metal AM with respect to conventional processes, including high flexibility in the production of complex shapes and highly customized parts, benefits at the supply chain reconfiguration level, and positive impacts on overall product life-cycle and value chain. The possibility of completely re-thinking the way high-value-added products are made – together with the capability of embedding new functionalities into the products,

introducing new material properties, and extending current business perspectives – represents a strategic issue for various industrial sectors, from aerospace to health-care, and from tooling and moulding to creative industries.

Mellor *et al*. (2014) presented a framework analysis for the implementation of AM showing that the implementation success is considerably influenced by the ability and will to change a traditional production culture. From an economic viability viewpoint, the integration of AM processes into existing or new production environments imposes the need for a reliable economic model to facilitate trade-off analyses and investment decisions. The ability to forecast the cost of an additively produced part is crucial to many company activities, not only at price setting or production planning levels, but also during the pre-development and concept design phases, where both the technological and economic suitability of new manufacturing solutions must be taken into account. Because of this, the mainstream literature has been increasingly focused on the development of cost models for AM (Thomas and Gilbert, 2014; Baumers *et al*., 2015; Laureijs *et al*., 2016; Huang *et al*., 2017). All the aforementioned models shared the common goal of quantitatively determining whether and to what extent metal AM is economically convenient compared to traditional technologies (e.g., casting and machining). Moreover, all of those studies implicitly assumed that defect-free parts are produced. Indeed, they did account for issues related to limited stability and repeatability of metal AM processes, which have been pointed out as being major technological barriers for the breakthrough exploitation of metal AM systems in industry (Thomas-Seale *et al*., 2018; Weller *et al*., 2015; Mani *et al*., 2015; Tapia and Elwany, 2014; Everton *et al*., 2016; Spears, 2015; Sames *et al*., 2016). Typical defects include internal and surface/sub-surface porosity, balling effects, cracks and delamination, geometrical and dimensional errors, and impurities and discontinuities at the microstructural level (Grasso and Colosimo, 2017). Because of this, increasing research and industrial development interest has been devoted to in-situ monitoring solutions in order to detect the onset of defects during the layerwise build of the part and to stop the process when needed to reduce the waste of material, time, and energy (Mani *et al*., 2015; Tapia and Elwany, 2014; Everton *et al*., 2016). Here, the term "in-situ monitoring" refers to the capability to automatically detect/localize defects and stop the process (i.e., suppress the defective part) when some defect-related quantities measured via in-situ sensors violate a given alarm threshold. All major metal AM system developers are equipping their systems with integrated sensing and monitoring tools (the reader

is referred to Appendix A for a summary of commercially available tools and the mainstream literature in this field). The AM processes where most off-the-shelf monitoring solutions are available are powder bed fusion (PBF) processes, which include laser-based PBF (LPBF) and electron beam melting (EBM). PBF processes represent the domain of interest for this study as they allow a higher feature resolution and accuracy than other metal AM processes at the expense of deposition rates and maximum build dimensions (Gibson *et al.*, 2010). This makes the PBF technology suitable for precision metal AM applications, where the impact of defects is more critical and in-situ monitoring represents a key enabling technology.

Despite the rapidly increasing number of studies and off-the-shelf toolkits for in-situ sensing and monitoring, there is a lack of studies quantifying the economic convenience of these solutions related to specific industrial applications. This study presents the first cost model aimed at filling this lack, as it offers a novel perspective on cost model analysis. Indeed, rather than quantifying the costs of metal AM for comparisons against traditional manufacturing alternatives, this study aims to generalize cost modelling formulations to determine (i) the economic impact of defects in metal LPBF processes and (ii) the extent to which in-situ monitoring tools are viable and economically convenient. To this aim, the proposed model extends previous cost modelling formulations available in the literature, introducing novel features needed to characterize the monitoring methodology performances on part production costs. Such performances are expressed in terms of false alarm rates (Type I error) and false negative rates (Type II error or number of actual defects that are not detected). In the common industrial practice, monitoring systems that produce high false alarm rates are usually switched off by the operator. The ability to estimate the actual economic impact of false alarms on the overall production costs is therefore essential to determine the convenience of added sensing and monitoring functionalities for advanced manufacturing applications. In this framework, the proposed model can be used to not only assess the relevance of fast in-line defect detection in the development of next generation metal AM systems, but it can also be used to define performance specifications of in-situ monitoring solutions that yield sustainable cost savings in applications of industrial interest. As such, three case studies from different industrial sectors (aerospace, dental and machinery) were assessed to explore how economic convenience can vary depending on the specific product features.

The remainder of the paper is organized as follows: Section 2 presents the cost model formulation, Section 3 describes three case studies related to three different industrial AM productions used to

demonstrate the practical use and potentials of the proposed model, Section 4 discusses the results achieved by applying the proposed cost model, Section 5 presents a validation analysis and Section 6 concludes the paper.

The spreadsheet for the implementation and test of our proposed cost model is made available by the authors upon request.

## 2. COST MODEL FORMULATION

### *2.1 State-of-the-art on cost models for AM*

The first seminal studies on AM cost modelling proposed generic models with a particular focus on rapid prototyping applications (Alexander *et al*., 1998) and series production of polymer parts (Hokinson and Dickens, 2003; Ruffo *et al*., 2006-2007). In the framework of metal AM, Atzeni and Salmi (2012) presented a cost model aimed at evaluating if AM technologies could be considered an economically convenient alternative to conventional processes for metal parts. Atzeni and Salmi (2012) presented a re-design analysis of an aerospace part and compared the viability of metal AM against high-pressure die-casting (HPDC). They demonstrated that AM was convenient for low production volumes leading to a considerably lower time to market. Lindemann *et al*. (2012) presented an analysis that accounted for all product lifecycle costs. Rather than presenting a cost model formulation, Lindemann *et al*. (2012) studied the main cost drivers and their impact on the cost of a single part by assessing a case study from the automotive sector. A new cost model for LPBF processes was presented by Rickenbacher *et al*. (2013), who devoted particular focus to pre- and post-processing operations. In their model, Rickenbacher *et al*. (2013) assumed that parts with different geometries could be included into the same build. The resulting model generalized and extended previously presented formulations. A generic cost model suitable for manufacturing applications was described previously (Ashby, 1999). Hart (2015) utilized this model to investigate the economic convenience of LPBF processes and included an additional factor, i.e., the value of the product, which took into account all non-economic benefits provided by metal AM systems. All the aforementioned models aim to determine whether and to what extent metal AM is economically convenient compared to traditional technologies. This study addresses the cost modelling issue in AM from a different perspective. In particular, the cost model

here presented is based on a cost breakdown structure that inherits the model framework presented by Rickenbacher *et al*. (2013) and Ashby (1999), but it extends previous formulations to evaluate the impact of process defectiveness and in-situ monitoring capabilities on production costs.

### *2.2 Proposed cost model*

The proposed cost model relies on a cost-breakdown structure driven by the major phases of the LPBF production workflow. It includes three sequential steps: (i) pre-process operations, aimed at carrying out the build[1] preparation and making the system ready to build; (ii) the LPBF process, during which the part is produced; and (iii) post-process operations aimed at extracting, inspecting, and post-processing the parts.

During the pre-process phase, a CAD model of each part is provided as input. The model is imported into a software for AM build preparation and the operator decides how to orient each part and support it. Eventually, the slicing operation is applied and a so-called "material file" or "process theme" is associated to each part in the build to define the process parameters and scan strategies to be used. In this phase, the LPBF system setup is performed, which includes different operations (e.g., chamber cleaning, filter substitution, powder refill, etc.) needed to bring the system into ready-to-print mode.

During the LPBF process, no human supervision is needed apart from periodic manual interventions to refill powder if and when required. After the process, the build must be extracted from the chamber and the excess powder must be recovered for subsequent sieving and recycling. The parts are then cut from the baseplate, inspected, and post-processed according to functional requirements. Post-processing operations may include surface finishing, machining of specific features, and thermal treatments.

The cost of a part, $C_{part}$, in discrete manufacturing productions can be estimated based on the cost model approach presented by Ashby (1999). Its generalization to metal AM (Rickenbacker et al., 2013; Hart, 2015) is defined as the sum of costs associated to three phases: the pre-process cost, $C_{pre}$; the LPBF process cost, $C_{proc}$, and the post-process cost, $C_{post}$. There is also a fourth term consisting of the cost of material, $C_{material}$. As such, $C_{part}$ can be expressed as follows (Rickenbacker et al., 2013):

$$C_{part} = C_{material} + C_{pre} + C_{proc} + C_{post} \quad (€/\text{part}) \tag{1}$$

[1] The terms "build" and "job" are used in industry and in the literature to indicate the stack of parts produced via LPBF in one single process run.

The proposed cost model relies on the following main assumptions:

- Each build includes a fixed number of parts.
- All the parts belong to the same category of product; they can be customized in shape and characteristics, but they have similar volume, height, and orientation within the build. This assumption is compliant with various industrial AM applications, such as aerospace and biomedical applications, where each LPBF system may be devoted to a specific type of product.
- In-situ monitoring tools are integrated into the LPBF system. This assumption can be easily relaxed by introducing an extra equipment cost, which depends on the type of sensors and the capabilities of the in-situ monitoring tool (see Section 4 for an analysis of the impact of such extra costs).
- No in-situ defect repair or feedback control is foreseen. This assumption reflects the current state-of-the-art of LPBF systems. Thus, we assume that, as a consequence of an in-situ defect detection, the only action available consists of stopping the process of defective parts while processing of the other parts in the same build goes on.

In this study, the cost for producing a part via LPBF was examined in three different scenarios. The first, namely *as-is* scenario, is representative of a real process with state-of-the-art LPBF technology in the absence of any in-situ defect detection capability. In the second scenario, labeled *monitoring* scenario, we assumed that the system is able to automatically stop processing a part once a defect has been detected by relying on in-situ gathered data. Notice that, in this case, the production of a part can be stopped as a consequence of a false alarm too. In the third scenario, the *monitoring & diagnosis* scenario, we assumed that whenever an alarm is signaled, the process can be paused and a human operator is called to carry out a diagnostic analysis based on available data and visual inspections. If the operator decides that the monitoring tool signaled a false alarm the process can go on, otherwise the part would be excluded from further processing. For sake of simplicity, the operator's diagnosis is assumed to be fully reliable in this last scenario.

### *2.2.1 Net cost, scrap cost and actual cost*

In the *as-is* scenario, the cost for producing a conforming part is inflated by the scrap fraction, $\gamma \in [0,1]$, where the term "scrap" refers to a defective part that can not be recovered via post-process treatments and hence it is a part to be wasted. Thus, the scrap fraction represents the failure rate of the AM process. The

larger the scrap fraction is, the larger the material waste is and the higher the LPBF process costs are because a larger number of parts must be produced to achieve the target number of conforming products. The pre-process cost is also affected by the scrap fraction because it includes build preparation and system setup costs that depend on how many process runs are globally needed. Regarding post-process costs, $C_{post}$ is the cost of the operations applied to every produced part (i.e., the cost of cutting the part from the baseplate and following quality inspections and measurements). Other application-dependent post-processing costs were not included here, but they could be added as extra costs to the present model.

Therefore, the effect of the scrap fraction, $\gamma$, on the unitary cost of a part can be determined as follows (Ashby, 1999):

$$C_{part} = \frac{C_{material}+C_{pre}+C_{proc}+C_{post}}{1-\gamma} \quad (€/\text{part}) \tag{2}$$

We let $C_{net} = C_{material} + C_{pre} + C_{proc} + C_{post}$ be the net cost for producing a conforming part with the only exception of extra (if needed) post-processing treatment costs. Thus, $C_{part} = \frac{C_{net}}{1-\gamma}$. Expression (2) can be generalized in the *monitoring* scenario (Montgomery, 2009). First, it was assumed that a perfect in-situ monitoring tool was available such that Type I error (false alarm rate) was $\alpha = 0$, and Type II error (false negative rate) was $\beta = 0$. Specifically,when a defect is present,it is always detected and no false alarms were produced. We let $C_{scrap}$ be the cost of producing a defective part. The scrap cost is defined as follows:

$$C_{scrap} = CR(C_{material} + C_{proc}) + C_{pre} + C_{post} \quad (€/\text{part}) \tag{3}$$

where $CR \in [0,1]$ is the "completion rate" and is equal to the fraction of the part produced before its production was stopped. For example, $CR = 0.5$ means that only 50% of the overall number of layers needed to produce the part was actually printed. Generally speaking, $C_{scrap} < C_{net}$ when layerwise part production is interrupted before the end of the process ($CR < 1$). Moreover, we let $\gamma$ be the probability that the part is a scrap and $1 - \gamma$ be the probability that the part is a non-defective one so that the actual cost can be generalized as follows:

$$C_{part} = \frac{(1-\gamma)C_{net}+\gamma C_{scrap}}{1-\gamma} \quad (€/\text{part}) \tag{4}$$

Eq. (4) is a generalization of the model presented by Ashby (1999), where the net cost of a part is different from the cost of producing a scrap like in the present case, because of an anticipated process interruption driven by the in-situ monitoring tool.

If $CR = 1$ (i.e., no anticipated process stop, which also corresponds to lack of in-situ monitoring capabilities), $C_{scrap} = C_{net}$ and Expression (4) simplifies to $C_{part} = \frac{C_{net}}{1-\gamma}$ (Ashby, 1999).

Expression (4) can be further generalized by considering that in-situ monitoring tools have no perfect performances (i.e., $\alpha \in [0,1]$ and $\beta \in [0,1]$). In the most general case, a conforming part could be wrongly classified as a scrap with probability $\alpha$, or it could be properly classified as a conforming one with probability $1-\alpha$. On the other hand, a scrap could be properly classified as a scrap with probability $1-\beta$ or wrongly classified as a conforming one with probability $\beta$. These possibilities are summarized in Fig. 1.

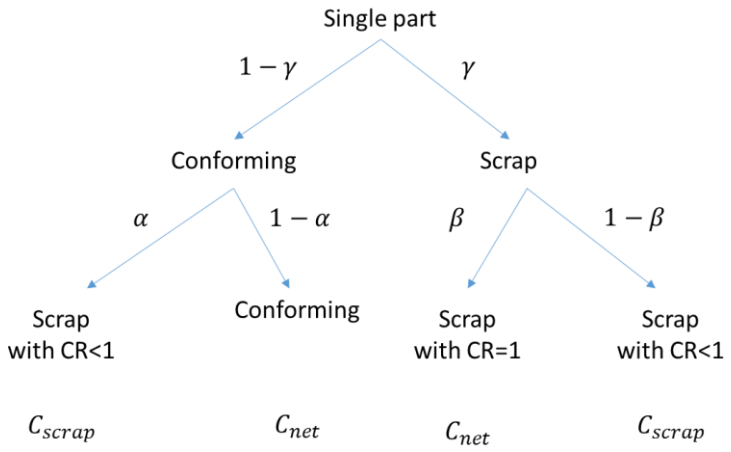


Fig. 1 – Net and scrap costs in the *monitoring* scenario depends on scrap fraction, $\gamma$, Type I error, $\alpha$, and Type II error, $\beta$

Notice that, in this case, $C_{scrap}$ could either be the cost of the actual scrap or the cost of a prematurely suppressed part as a consequence of a false alarm. Therefore, Expression (4) could be generalized as follows, by taking into consideration Type I and Type II errors from the in-situ monitoring tool:

$$C_{part} = \frac{(1-\gamma)\left[\frac{(1-\alpha)C_{net}+\alpha C_{scrap}}{1-\alpha}\right]+(\gamma)[\beta C_{net}+(1-\beta)C_{scrap}]}{1-\gamma} \quad (€/\text{part}) \tag{5}$$

Eq. (5) merges the effect of scraps on overall part costs based on Ashby (1999), with the method traditionally used in statistical process control to evaluate the effect of Type I and Type II errors (Montgomery, 2009).

A few special cases could be considered:

- When $\alpha = 0$ and $\beta = 1$, the in-situ monitoring tool has no effect, thus $CR = 1$ for all the parts. This is equivalent to the *as-is* scenario where no in-situ monitoring capability is envisaged. In this case, Expression (5) reduces to $C_{part} = \frac{C_{net}}{1-\gamma}$;
- When $\gamma = 0$ (no actual defects) but $\alpha \neq 0$ and $\beta \neq 0$, Expression (5) reduces to $C_{part} = \frac{(1-\alpha)C_{net}+\alpha C_{scrap}}{1-\alpha}$, or all scraps are prematurely suppressed parts caused by false alarms.

When the monitoring system signals an alarm in the *monitoring & diagnosis* scenario, the process is paused and a diagnosis analysis is performed. In this case, we assumed that the human operator may have analysed the acquired data and decide whether or not the alarm was a false one. There are two differences with respect to the *monitoring* scenario. First, thanks to the on-line diagnosis step, false alarms do not result in part suppression. Second, this scenario has to account for an extra cost, $C_{extra}$, which is proportional to the time needed to perform the diagnosis analysis before re-starting the process. Having assumed a fully reliable diagnosis, a conforming part could never be wrongly classified as a scrap. However, the extra cost, $C_{extra}$, has to be added to the net cost, $C_{net}$, with probability $\alpha$ as a consequence of false alarms. On the other hand, a scrap could be properly classified as a scrap with probability $1 - \beta$, but the extra cost has to be added to the scrap cost. Otherwise, the scrap would be wrongly classified as a conforming one with probability $\beta$, and no process interruption would have occurred in this case. These possibilities are summarized in Fig. 2.

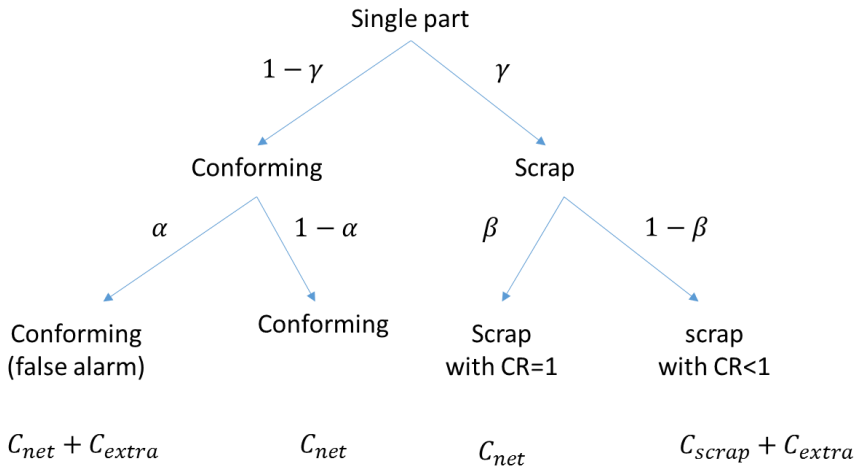


Fig.2 – Net and scrap costs in the *monitoring & diagnosis* scenario depends on scrap fraction, $\gamma$, Type I error, $\alpha$, and Type II error, $\beta$

In the *monitoring & diagnosis* scenario, the actual cost of a part can be computed as follows:

$$C_{part} = \frac{(1-\gamma)[(1-\alpha)C_{net} + \alpha(C_{net} + C_{extra})] + (\gamma)\left[\beta C_{net} + (1-\beta)\left(C_{scrap} + C_{extra}\right)\right]}{1-\gamma} = \\ = \frac{(1-\gamma)[C_{net}+\alpha C_{extra}]+(\gamma)\left[\beta C_{net}+(1-\beta)\left(C_{scrap}+C_{extra}\right)\right]}{1-\gamma} \text{ (€/part)} \quad (6)$$

Eq. (6) generalized eq. (5) when false alarms yield only an extra cost associated to the diagnosis phase rather than leading to extra costs due to an undesired interruption of the process for a conforming part.

A few special cases can be considered also in this case:

- When $\alpha = 0$ and $\beta = 1$, the in-situ monitoring tool has no effect, thus $CR = 1$ for all the parts and Expression (6) reduces to $C_{part} = \frac{C_{net}}{1-\gamma}$.
- When $\alpha = 0$ and $\beta = 0$, the in-situ monitoring tool performs perfectly, thus Expression (6) reduces to $C_{part} = \frac{(1-\gamma)C_{net}+\gamma(C_{scrap}+C_{extra})}{1-\gamma}$.
- When $\gamma = 0$ (no actual defects) but $\alpha \neq 0$ and $\beta \neq 0$, Expression (6) reduces to $C_{part} = C_{net} + \alpha C_{extra}$, so the extra cost must be added to the net cost with probability equal to the false alarm rate.

Table 1 summarizes the $C_{part}$ expression in the three scenarios examined in this study.

Table 1 – Summary of expressions for the actual part cost in different scenarios

| **Scenario** | **Actual cost formulation** |
|---|---|
| *As-is* | $C_{part} = \frac{C_{net}}{1-\gamma}$ |
| *Monitoring* | $C_{part} = \frac{(1-\gamma)\left[\frac{(1-\alpha)C_{net} + \alpha C_{scrap}}{1-\alpha}\right] + (\gamma)\left[\beta C_{net} + (1-\beta)C_{scrap}\right]}{1-\gamma}$ |
| *Monitoring & diagnosis* | $C_{part} = \frac{(1-\gamma)[C_{net} + \alpha C_{extra}] + (\gamma)\left[\beta C_{net} + (1-\beta)\left(C_{scrap} + C_{extra}\right)\right]}{1-\gamma}$ |

The formulation of each cost model term is briefly discussed in sub-section 2.2.2 to 2.2.5.

### *2.2.2 Material cost*

According to the model discussed by Hart (2015), the cost of the material, $C_{material}$, is defined as follows:

$$C_{material} = P_{price} V \rho (1 + w) \text{ (€/part)}, \quad (7)$$

where:

$P_{price}$: price of the metal powder (€/kg).

$V$: volume of the part ($m^3$).

$\rho$: density of the solid material ($kg/m^3$).

$w$: ratio of material not recycled at the end of the process (-).

### *2.2.3 Pre-process cost*

Pre-processing costs can be expressed as a sum of two terms: the cost related to the preparation of the build where the part is included and the cost related to the setup of the LPBF system before starting the process. In this study, we assumed that the CAD model was an input whose development cost was not included into the production cost estimation. According to Rickenbacher *et al*. (2013), the pre-processing cost is defined as follows:

$$C_{pre} = C_{buildprep} + C_{setup} \quad (€/part), \tag{8}$$

$$C_{jobprep} = \frac{(C_{operator} + C_{PC})T_{buildprep}}{n_p} \tag{9}$$

$$C_{setup} = \frac{(C_{operator} + C_{LPBFsys})T_{setup}}{n_p} \tag{10}$$

where:

$C_{operator}$: hourly operator cost (€/h).

$C_{PC}$: hourly cost for workstation and software use (€/h).

$C_{buildprep}$: cost for the preparation of the build, where the part is included, divided by the number of parts in the same build (€/part).

$T_{buildprep}$: time needed for the build preparation (h).

$n_p$: number of parts in the same build (-).

$C_{setup}$: cost for the LPBF system setup before the process divided by the number of parts in the same build (€/part).

$C_{LPBFsys}$: hourly cost of the LPBF system (€/h).

$T_{setup}$: time needed for the LPBF system setup before the process (h).

The hourly cost of the LPBF system, $C_{LPBFsys}$, could be computed by assuming depreciation over a given number of years (using a straight-line depreciation) and including fixed maintenance and space rental costs according to Ashby (1999).

### *2.2.4 LPBF process cost*

The LPBF processing cost is determined by hourly cost of the LPBF system, $C_{LPBFsys}$, energy consumption cost, $C_{energy}$, and inert gas consumption cost, $C_{inertgas}$, multiplied by the duration of the process. It is defined as follows, according to Rickenbacher *et al*. (2013):

$$C_{proc} = \frac{(C_{energy}+C_{inertgas}+C_{LPBFsys})T_{build}}{n_p} \quad (€/\text{part}) \tag{11}$$

where:

$C_{energy}$: hourly cost of the LPBF system energy consumption (€/h).

$C_{inertgas}$: hourly cost of the inert gas consumption during the process (€/h).

$T_{build}$: time needed to complete the build (h).

### *2.2.5 Post-process cost*

Generally speaking, post-processing operations can be divided into two categories: (i) operations applied to all the parts, both defective and non-defective ones, and (ii) operations applied only to non-defective parts after quality inspections. The latter category, e.g., surface finishing operations, represents a cost term not affected by the scrap fraction (assuming that a crap is a part whose defects can not be recovered or corrected by those operations). Thus, it is not included into the following model formulation, but it can be added as an application-dependent extra cost. The former category, instead, includes the costs for the removal of the parts from the LPBF system, cutting parts from the baseplate, and quality inspections and measurements. All these costs are included in the term $C_{post}$. According to the assumptions stated above and the cost model formulation of Rickenbacher *et al*. (2013), the post-process cost is defined as follows:

$$C_{post} = C_{removal} + C_{basecut} + C_{inspection} \quad (€/\text{part}) \tag{12}$$

$$C_{removal} = \frac{(C_{operator} + C_{LPBFsys})T_{removal}}{n_p} \tag{13}$$

$$C_{basecut} = (C_{cut}/A_{baseplate})A_{part} \tag{14}$$

$$C_{inspection} = \left(C_{operator} + C_{measurement}\right)T_{inpsection} \quad (15)$$

where:

$C_{removal}$: cost for the removal of the build from the LPBF system, divided by the number of parts in the same build (€/part).

$C_{post}$: cost of post-process operations applied to all the produced parts (€/part).

$T_{removal}$: time needed to remove the build from the LPBF systems (h).

$C_{basecut}$: cost for cutting the part from the baseplate (€/part).

$C_{cut}$: cost for cutting an area equal to the baseplate surface (€/build).

$A_{baseplate}$: area of the baseplate ($m^2$).

$A_{part}$: area of the interface between the part and the baseplate ($m^2$).

$C_{inspection}$: cost for the quality inspection of the part (€/part).

$C_{measurement}$: hourly cost of the metrological equipment used for the quality inspection (€/h).

$T_{inpsection}$: time needed to inspect one part (h).

### *2.2.6 Production time estimation*

The model formulation presented so far could be easily adapted to compute the average time to produce a part, including the time devoted to pre- and post-process operations. Table 3 summarizes the expressions for production time calculation, derived from the ones reported in Table 2, where:

$$T_{net} = T_{pre} + T_{proc} + T_{post} \text{ (h/part)} \quad (16)$$

$$T_{scrap} = CR * T_{proc} + T_{pre} + T_{post} \text{ (h/part)} \quad (17)$$

$T_{pre}$, $T_{proc}$ and $T_{post}$ are respectively the time devoted to pre-processing operations for each part, part production via LPBF, and post-processing operations on the part. In the *monitoring & diagnosis* scenario, $T_{diagnosis}$ stood for the time needed to carry out the diagnosis step once an alarm has been signaled by the in-situ monitoring tool. Expressions in Table 2 are based on the same principle of part cost models in Table 1, and they rely on the traditional way of evaluating Type I and Type II errors in statistical process control (Montgomery, 2009).

Table 2 – Summary of expressions for evaluating part production time in different scenarios

| Scenario | Actual cost formulation |
|---|---|
| *As-is* | $T_{part} = \frac{T_{net}}{1-\gamma}$ |
| *Monitoring* | $T_{part} = \frac{(1-\gamma)\left[\frac{(1-\alpha)T_{net} + \alpha T_{scrap}}{1-\alpha}\right] + (\gamma)\left[\beta T_{net} + (1-\beta)T_{scrap}\right]}{1-\gamma}$ |
| *Monitoring & diagnosis* | $T_{part} = \frac{(1-\gamma)\left[T_{net} + \alpha T_{diagnosis}\right] + (\gamma)\left[\beta T_{net} + (1-\beta)\left(T_{scrap} + T_{diagnosis}\right)\right]}{1-\gamma}$ |

### *2.2.7 On model generalization to other AM processes*

The proposed cost modelling framework was conceived for LPBF, but to some extent it can be generalized to other metal AM processes. One possible extension regards EBM processes, i.e., PBF processes where a high speed electron beam is used to pre-heat and selectively melt a powder bed on a layer-by-layer basis. The following guidelines should be used to extend the proposed model to EBM:

i) The $C_{LPBFsys}$term, to be renamed $C_{EBMsys}$, should represent the EBM system hourly cost;

ii) The $C_{removal}$ term should include also the cost of the additional equipment needed for removing the sintered powder and extracting the built parts (i.e., the powder recovery system);

iii) The $C_{basecut}$ can be set to 0 in most EBM applications, as the parts can be easily removed by hands from the baseplate in most cases;

iv) The $T_{build}$ term should include not only the actual EBM process duration, but also the following cooling phase duration, typical of EBM processes.

In order to generalize the proposed cost model to other AM processes, additional modifications might be applied. The cost decomposition in Eq. 1 is applicable to any metal AM application, but each cost term should be tailored to the specific technology. The net and scarp cost definition framework shown in Fig. 1 and Fig. 2 is applicable to other technologies too, together with the way in-situ monitoring cost evaluations based on false positive and false negative performances are embedded into the model.

Generally speaking, once material, process, pre- and post-processing costs have been modelled depending on the specific technology, the proposed approach for the quantification of the economic convenience of in-situ monitoring methods can still be applied without relevant modifications to every metal AM applications where in-situ defect detection and consequent process interruption is feasible.

## 3. CASE STUDIES FOR MODEL PERFORMANCE ANALYSIS

### *3.1 Overview and motivation of selected case studies*

Three case studies were selected in order to evaluate the proposed cost model. Their choice was driven by the following inclusion and exclusion criteria (Yin, 2009):

- Inclusion criteria: they are representative of the three industrial sectors with the highest technology readiness level (TRL) in metal AM (Langefeld, 2013, Wholers, 2018), i.e., dental, aerospace and machinery & tooling. These three sectors are also the ones where series production via metal AM are more consolidated and already available on the market (Wholers, 2018). Moreover, the three selected case studies represent three different categories of products, namely low-, medium-, and high-value-added metal AM parts. Indeed they involve three different categories of material costs, three different process durations (from few hours to one day and a half), three different part dimensions and three different geometry complexity levels. They involve, respectively, the production of dental prostheses in cobalt chrome (case study 1), a machinery component in stainless steel (case study 2) and an aerospace bracket in Ti6Al4V (case study 3). The main features and differences between these three cases are summarized in Table 3.
- Exclusion criteria: we excluded from the case study selection parts from industrial sectors with lower TRL in metal AM (Langefeld, 2013; Wholers, 2018), where series production is still not consolidated or not available of the market. In particular, we excluded rapid prototyping applications, since the proposed model is specifically design for series productions.

Table 3 – Main characteristics and salient features of the three case studies.

| **Characteristic** | **Dental prostheses production** | **Machinery component** | **Aerospace bracket** |
|---|---|---|---|
| Material | Cobalt chrome | Stainless steel | Ti6Al4V |
| Complexity | Low | Medium | Medium/high |
| Dimensions | Small ($V$=6*10$^{-6}$ m$^3$) | Medium ($V$=3.7*10$^{-5}$ m$^3$) | Large ($V$=7.35*10$^{-5}$ m$^3$) |
| Scrap ratio | Low (<0.1) | Medium-high (0.2 ÷ 0.4) | Medium-high (>0.2) |
| Processing time | Low (7 h/build) | Medium (26 h/build) | High (36 h/build) |
| Quality inspections | Manual controls and visual inspection | CMM measurement (possibly CT-scan for lattice structure inspection) | CMM measurement |
| AM production in market | Consolidate production | New product | New product |

The first case study regards the production of dental prostheses in cobalt chrome. PBF processes have become a quite consolidated technology in the dental sector thanks to their flexibility to produce customized implants with a lower delivery time than conventional approaches (Berger, 2013). Indeed, the technology readiness level in the dental sector is one of the highest (i.e., about 9 - 10 on a scale that ranges from 1 to 10) among the most relevant application sectors for metal AM[2]. In this framework, LPBF is suitable to produce fully integrated dental solutions, including crowns, bridges, and removable partial dentures, with certified medical materials. This kind of application involves the production of small parts (e.g., build heights in the range 10 – 50 mm) that are similar in dimension and complexity but customizable in shape (Fig. 3, left panel). Each build may include several parts, and a company may produce hundreds or thousands of builds per year to face a continuously increasing market demand. The processing time is quite low, and all the parts included in one build may be ready for use in a short time. Typical scrap fractions are quite low too (e.g., less than 0.1) (EOS web site). Regarding the quality inspection of dental prostheses, we assumed that operators carry out manual controls and visual inspections, although more accurate inspections can be applied (e.g., metrological characterization via coordinate measurement machines - CMMs).

The second case study regards the production of a machinery component that has been re-designed to be produced via LPBF of stainless steel by exploiting a cellular lattice structure for weight reduction with no detrimental effects on the functional and mechanical properties of the part. It was representative of novel metal AM applications in which complex products are partially or completely re-designed to implement metal AM into existing production frameworks. The part that was used as a reference for this second case study is shown in Fig. 3 (central panel).

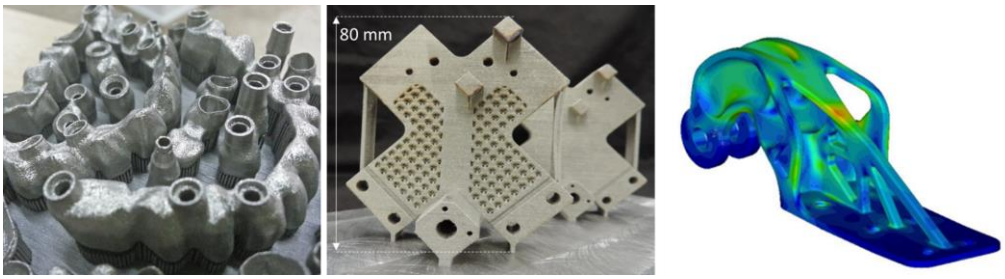


Fig. 3 – Left panel: example of dental prosthesis produced via LBPF; central panel: machinery component produced via LPBF; right panel: 3D representation of topologically optimized aerospace bracket (Tomlin and Mayer, 2011)

[2] https://www.rolandberger.com/en/Publications/pub_additive_manufacturing_2013.html

The complexity of the part is higher than in the previous case study due to the presence of the lattice structure, a combination of filled volumes and trabecular structures together with large overhanging areas. The height of the part is about 80 mm and the volume is about $3.7*10^{-5}$ $m^3$. Compared to the dental prostheses case, the product in the second case study results in lower number of parts per build, a considerably longer production time (about 26 hours using stainless steel powder when four parts per build are produced on a single-beam LPBF system), and higher expected scrap fractions (between 0.2 and 0.3) caused by the higher complexity of the part. The part is inspected via a CMM for dimensional and shape measurements. Additional costs for Computer Tomography (CT) scans of the lattice structure may be considered too, but they were not included in the present computation.

The last case study, which is representative of topologically optimized structural components for aerospace applications, was taken from the work of Tomlin and Meyer (2011) on the re-design of an Airbus A320 nacelle hinge bracket produced via LPBF (Fig. 3, right panel). The part has a larger volume than the machinery component in the second case study (about $7.35*10^{-5}$ $m^3$), which leads to a larger build time in the order of 36 h after having assumed a build rate of 18 $cm^3$/h and two parts per build. The bracket was manufactured in Ti6Al4V, which also results in a considerably higher material cost ($P_{price} = 320\ €/kg$). These issues make the occurrence of defects particularly critical and highly economically impactful.

In addition to inclusion and exclusion criteria mentioned above, the choice of these three case studies was driven by the following criteria (Yin, 2009):

- Internal validity: all case studies presented in the paper refer to real industrial cases with settings based on literature data and/or previous manufacturing experience, and hence there is no risk to introduce spurious data.
- External validity: the cost basis estimation in our model grounds the one presented in Ashby (1999). This was model framework was used and generalized to AM by other authors (e.g., Hart 2015, Rickenbacher et al., 2013). We merged such generalizations with reference methods to evaluate the performances of statistical process monitoring tools (Montgomery, 2009). Moreover, the proposed cost model relies on clearly stated assumptions, it includes no black-box estimation, no implicit or hidden

function. Therefore, it is directly applicable to case studies in metal AM that are different from the ones here presented.

- Reliability: all the data and model settings required to make the analysis repeatable are provided in the following. Input data for the case study 1 where provided by LPBF system developers[3] and integrated with information available in companies' websites (EOS web site). Regarding the case study 2, different copies of the same part were manufactured in our laboratory by means of a Renishaw AM250 system. Therefore, most of input data were based on direct manufacturing experience. Additional information (e.g., type and costs of quality inspections on this product) were provided by the company that commissioned the re-design of the part. Regarding the case study 3, input data were gathered from the literature (Tomlin and Mayer, 2011), and from our direct experience in producing copies of the same part.

Generally speaking, the construct validity of the analysis relies on the selection of three case studies representative of different industrial sectors belonging to three different categories of products, characterized by different characteristics, complexities and cost drivers. It also relies on the fact the proposed cost model grounds on clearly stated assumptions, without implicit or hidden function that could prevent from replicating part of the results here presented. Input data for cost model evaluations are based on the literature, on direct manufacturing experience or inputs provided by AM companies. The lack of hidden function and assumptions make it applicable to other case studies in AM. To this aim, the spreadsheet that implements the presented model is made available by the authors upon request.

### *3.2 Model parameters*

The model parameters were divided into three categories: (i) constants, the values of which were kept fixed in all the scenarios; (ii) deterministic parameters, the values of which may vary depending on the specific scenario (*as-is*, *monitoring*, or *monitoring & diagnosis*); and (iii) random parameters, which may be affected by uncertainty and their values are drawn from a given probability distribution in each scenario.

[3] All the companies interviewed during the development of the present study gave consent to the use of provided data and information.

Table 4 summarizes the values associated with each model input in all case studies. Regarding the dental and machinery case studies, input values were based on direct manufacturing experience and benchmark industrial values. Regarding the aerospace case study, model inputs were based on either literature data or direct manufacturing experience.

Table 4 – Values of constants and model inputs used in the three case studies.

| **Category** | **Parameter** | **Values** | | |
|---|---|---|---|---|
| | | **Dental prostheses** | **Machinery component** | **Aerospace bracket** |
| Constants | $P_{price}$ (€/kg) | 295 | 92 | 320 |
| | $V$ ($m^3$) | $6*10^{-6}$ | $3.7*10^{-5}$ | $7.35*10^{-5}$ |
| | $\rho$ ($kg/m^3$) | 8300 | 7980 | 4430 |
| | $w$ | 0.05 | | |
| | $C_{operator}$ (€/h) | 20 | | |
| | $C_{PC}$ (€/h) | 2.5 | | |
| | $T_{buildprep}$ (h) | 0.5 | | |
| | $n_p$ | 8 | 4 | 2 |
| | $C_{LPBFsys}$ (€/h) | 28 | | |
| | $C_{energy}$ (€/h) | 0.64 | | |
| | $C_{inertgas}$ (€/h) | 5 | | |
| | $C_{cut}$ (€/build) | 2 | | |
| | $A_{baseplate}$ ($m^2$) | 0.0625 | | |
| | $A_{part}$ ($m^2$) | $2.5*10^{-5}$ | $2.25*10^{-4}$ | $1*10^{-3}$ |
| | $C_{measurement}$ (€/h) | 0,5 | 5 | 5 |
| Deterministic parameters | $\alpha$ | As-is: $\alpha = 0$<br>Monitoring: $\alpha \in [0,..,0.05]$<br>Monitoring & diagnosis: $\alpha \in [0,..,0.05]$ | As-is: $\alpha = 0$<br>Monitoring: $\alpha \in [0,..,0.05]$<br>Monitoring & diagnosis: $\alpha \in [0,..,0.05]$ | As-is: $\alpha = 0$<br>Monitoring: $\alpha \in [0,..,0.05]$<br>Monitoring & diagnosis: $\alpha \in [0,..,0.05]$ |
| | $\beta$ | As-is: $\beta = 1$<br>Monitoring: $\beta \in [0,..,0.3]$<br>Monitoring & diagnosis: $\beta \in [0,..,0.3]$ | As-is: $\beta = 1$<br>Monitoring: $\beta \in [0,..,0.3]$<br>Monitoring & diagnosis: $\beta \in [0,..,0.3]$ | As-is: $\beta = 1$<br>Monitoring: $\beta \in [0,..,0.3]$<br>Monitoring & diagnosis: $\beta \in [0,..,0.3]$ |
| | $\gamma$ | $\gamma \in [0,..,0.2]$ | $\gamma \in [0,..,0.4]$ | $\gamma \in [0,..,0.4]$ |
| Random parameters | $CR$ | As-is: 1<br>Monitoring: $CR \sim U(0.1,0.9)$<br>Monitoring & diagnosis: $CR \sim U(0.1,0.9)$ | As-is: 1<br>Monitoring: $CR \sim U(0.1,0.9)$<br>Monitoring & diagnosis: $CR \sim U(0.1,0.9)$ | As-is: 1<br>Monitoring: $CR \sim U(0.1,0.9)$<br>Monitoring & diagnosis: $CR \sim U(0.1,0.9)$ |
| | $T_{setup}$ (h) | $T_{setup} \sim N(2,0.1)$ | $T_{setup} \sim N(2,0.1)$ | $T_{setup} \sim N(2,0.1)$ |
| | $T_{build}$ (h) | $T_{build} \sim N(7,0.1)$ | $T_{build} \sim N(26,0.2)$ | $T_{build} \sim N(36,0.3)$ |
| | $T_{removal}$ (h) | $T_{removal} \sim N(0.25,0.1)$ | $T_{removal} \sim N(0.5,0.2)$ | $T_{removal} \sim N(0.5,0.2)$ |
| | $T_{inspection}$ (h) | $T_{inspection} \sim N(0.5,0.1)$ | $T_{inspection} \sim N(2,0.2)$ | $T_{inspection} \sim N(2,0.2)$ |
| | $C_{extra}$ (€) | $C_{extra} \sim N(8,0.1)$ | | |

In the first case study, the production of complete removable dentures was considered, such that about eight parts per build could be manufactured. Generally speaking, we considered a powder recycling percentage of about 95% and referred to an LPBF system with a build area of 250 x 250 mm. The hourly LPBF system cost, $C_{LPBFsys}$, was based on the price for a new single-beam LPBF system of 600 k€. We also assumed depreciation was over 5 years (using a straight-line depreciation) from continuous use (load factor of 55%) and fixed maintenance (20 k€/year), and we considered space rental costs (600 €/year). The operator cost, $C_{operator}$, was set at 20 €/h, considering an average cost for low/medium skilled personnel. The hourly cost of HW/SW units, $C_{PC}$, was estimated by considering average licence prices of AM build design software products that are available off-the-shelf. The hourly costs of metrological inspections tools, $C_{measurement}$, were estimated based on the nature of inspections and operations required in the two case studies.

Different ranges of scrap fractions, $\gamma$, were considered: $\gamma \in [0,..,0.2]$ in the dental prostheses case and $\gamma \in [0,..,0.4]$ in the mechanical and aerospace component applications. In the former case, an average percentage of defective prostheses of about 10% was assumed, whereas in the latter two cases, the average defective percentage may have been larger (e.g., more than 20%) because of a higher part complexity and longer LPBF process. The cost for cutting the parts from the baseplate, $C_{cut}$, referred to the use of an in-house part removal technology (e.g., electrical discharge machining) and assumed that only supports with small cross-sections must be cut.

The time needed to prepare the build, $T_{buildprep}$, and the setup of the LPBF system, $T_{setup}$, were based on previous production experience. However, $T_{setup}$ was considered a random parameter drawn from a normal distribution with mean $\mu = 2$ h and standard deviation $\sigma = 0.1$ h, because it could vary from operator to operator. All the model parameters expressed as random variables were drawn from a normal distribution. The mean build time, $T_{build}$, was either based on the real time needed to produce a part or on the average build rate of an LPBF system with a single beam. The mean quality inspection time, $T_{inspection}$, was an estimate based on the nature of operations and measurements foreseen in the three case studies.

The completion rate, $CR$, was drawn from a uniform distribution with parameters 0.1 and 0.9. In the absence of additional information, this indicates that there was no single layer (or portions of layers) that was more critical than others in terms of probability of defect occurrence. If a priori information about the

defect probability was available, it could have been used to tune the reference distribution for the $CR$ parameter.

The extra cost for on-line diagnosis, $C_{extra}$, was estimated as follows:

$$C_{extra} = T_{diagnosis}(C_{operator} + C_{LPBFsys}) \quad (€/\text{part}) \tag{18}$$

where $T_{diagnosis}$ is the time needed to carry out the diagnosis analysis. We assumed an average time $T_{diagnosis} = 10\ min$ needed by the operator to visualize the acquired data, analyse the current status of the process, and make a decision. This yielded an average $C_{extra}$ cost of 8 €/part. We inserted this term into the model by drawing its value from a normal distribution of parameters $\mu = 8$ (€/part) and $\sigma = 0.1$ (€/part).

Regarding the performances of the in-situ monitoring tool, Type I ($\alpha$) and Type II ($\beta$) errors varied in range, $[0,..,0.05]$ and $[0,..,0.3]$, respectively. From a statistical process control perspective (Montgomery, 2009), Type I error could be controlled by properly designing the monitoring tool (e.g., $\alpha = 0.0027$ is a common design choice), whereas Type II error depends on the nature and the severity of the defect. An increase of Type I error with respect to the desired target may occur in the presence of violations of the assumptions adopted during the design of the alarm rule or when insufficient or not fully representative data are available to train the monitoring tool. A Type I error $\alpha = 0.05$ implies that 5% of the parts are aborted because of a false alarm, which is indicative of quite poor monitoring performance. On the other hand, a Type II error $\beta = 0.3$ implies that 30% of actual defects are not detected, which is indicative of quite low detection power. Thus, the selected intervals for these two kinds of errors ranged from high defect detection performances to quite poor ones.

## 4. DISCUSSION AND RESULTS

This section presents the results of Monte Carlo simulations aimed to compare part costs in the *as-is*, *monitoring*, and *monitoring & diagnosis* scenarios and evaluate the economic viability of in-situ monitoring tools in the metal AM case studies introduced in Section 3.

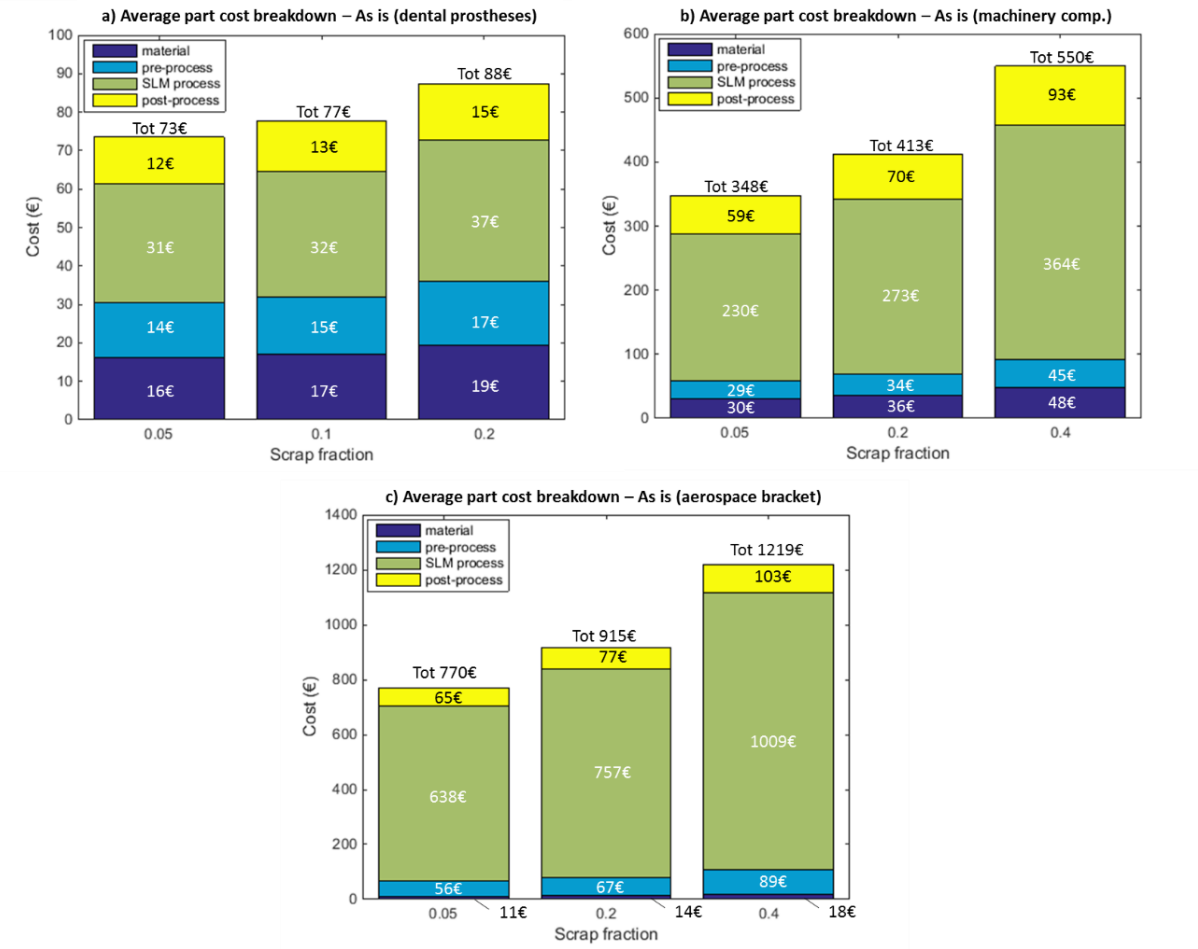


Fig. 4 – Average part cost breakdown in the dental prostheses case study (a), machinery component case study (b), and aerospace bracket case study (c) according to the *as-is* scenario

### *4.1 Cost model results*

We first outline the relative contribution of each cost model term to the overall cost of the part in the *as-is* scenario, depending on the scrap fraction. Fig. 4 shows the average part cost breakdown into the four main model terms for the dental prostheses (Fig. 4a), the machinery component (Fig. 4b), and the aerospace bracket (Fig. 4c) case studies, respectively. A cross-check of part costs in Fig. 4 was performed, based on interviews with the companies that provided input data related to case study 1 and 2, and with one of the largest AM service bureaus in Europe. Interviewed companies confirmed the correctness of the cost basis estimates with a margin of ±20%, depending on their internal policies for cost assessments.

In all cases, the LPBF process cost represented the major contribution to the unitary cost. In the dental prostheses case study (Fig. 4a), the LPBF process cost accounted for more than 42% of the overall part cost, whereas in the machinery component (Fig. 4b) and the aerospace bracket (Fig. 4c) case studies it accounted

for more than 66% and 82% of the overall part cost, respectively. The gap between these percentages is mainly due to different build durations, as the hourly cost of the LPBF system plays a primary role in the cost breakdown structure. A comparison between the part cost with and without in-situ monitoring capabilities (i.e., between the part costs in the *as-is* and the *monitoring* scenario) is shown for the three case studies in Fig. 5, Fig. 6, and Fig. 7. The part cost, with corresponding 95% Bonferroni's confidence intervals, is expressed as a function of the scrap fraction, $\gamma$, and the monitoring performances (each panel corresponds to a combination of $\alpha$ and $\beta$ error values). Fig. 5 to Fig. 7 demonstrate that when Type I error, $\alpha$, increases, the major effect on the part cost in the *monitoring* scenario consists of an increase of the vertical intercept of the cost curve, whereas an increase of Type II error, $\beta$, mainly causes a slight increase of the slope of the cost curve. This suggests that the false alarm rate, $\alpha$, is the most critical performance indicator. In the presence of false alarms, the process is interrupted prematurely with a consequent inflation of the overall cost, even when the scrap fraction was null or very low. The effect of Type II error, $\beta$, instead, depends on $\gamma$: the smaller the scrap fraction, the lower the benefit of in-situ monitoring with a low $\beta$ error.

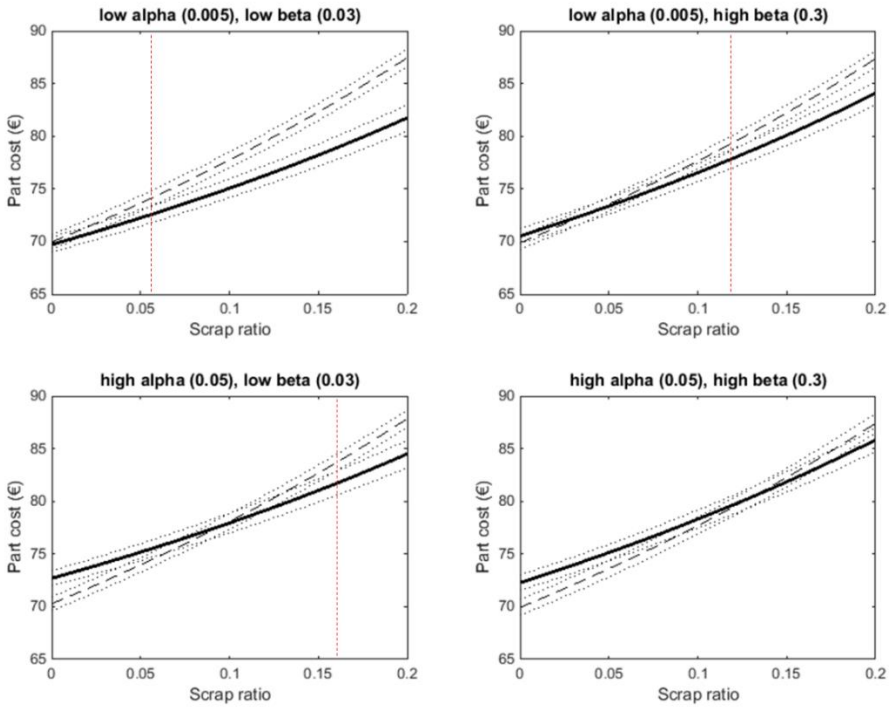


Fig. 5 – Dental prostheses case study: comparison of the part cost curve in the as-is scenario (dashed line) and the monitoring scenario (solid thick line) with 95% Bonferroni's confidence intervals (dotted lines) as a function of $\gamma$ for different in-situ monitoring performances; the vertical red dotted line corresponds to the upper intersection between the confidence envelopes

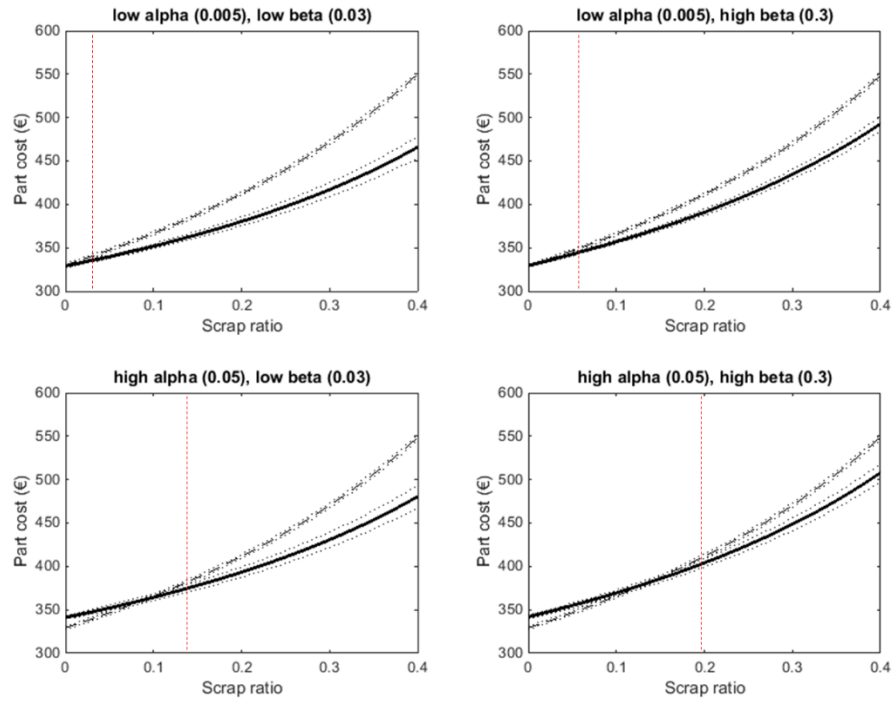


Fig. 6 – Machinery component case study: comparison of the part cost curve in the as-is scenario (dashed line) and the monitoring scenario (solid thick line) with 95% Bonferroni's confidence intervals (dotted lines) as a function of $\gamma$ for different in-situ monitoring performances; the vertical red dotted line corresponds to the upper intersection between the confidence envelopes

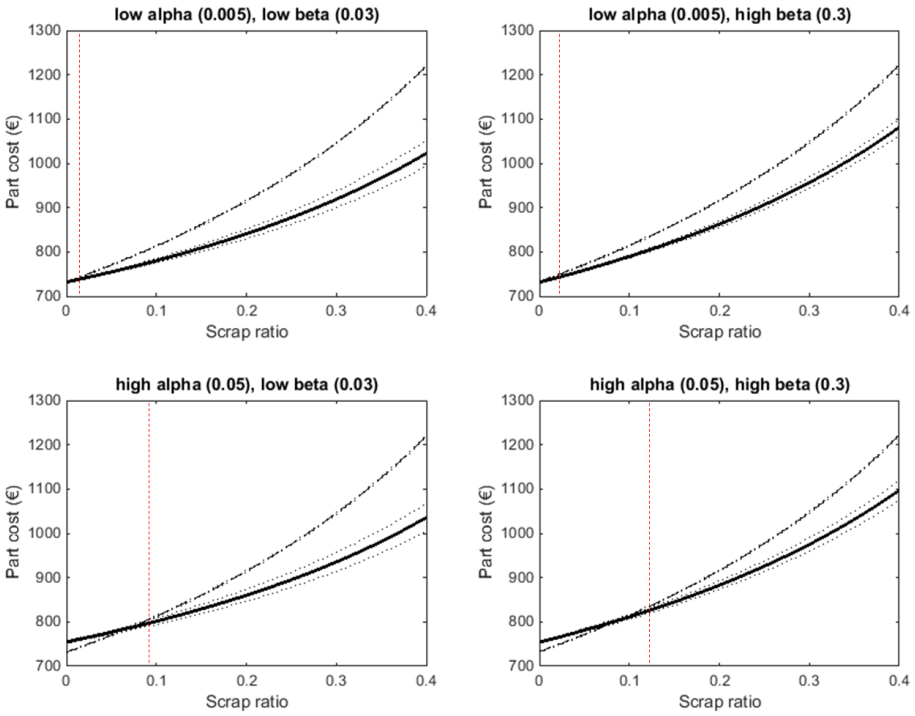


Fig. 7 – Aerospace bracket case study: comparison of the part cost curve in the as-is scenario (dashed line) and the monitoring scenario (solid thick line) with 95% Bonferroni's confidence intervals (dotted lines) as a function of $\gamma$ for different in-situ monitoring performances; the vertical red dotted line corresponds to the upper intersection between the confidence envelopes

More specifically, in the presence of a low duration LPBF process for relatively low cost and simple products (Fig. 5), the availability of an in-situ monitoring tool was economically convenient for $\gamma \leq 0.2$ in the presence of low false alarm rates or even with a high false alarm rate but a low false negative rate. For example, the minimum scrap fraction at which an in-situ monitoring tool with $\alpha = 0.005$ was economically convenient (at 95% confidence level) was about 0.06 (Fig. 5, top-left panel) and about 0.12 (Fig. 5, top-right panel) for $\beta = 0.03$ and $\beta = 0.3$, respectively. It is worth mentioning that statistical process monitoring methods are usually designed with an in-control false alarm error $\alpha = 0.0027$, which indicates that the two scenarios shown in the top panels of Fig. 5 were compatible with the state-of-the-art of process monitoring tools. However, when both the false alarm and false negative rates are high (i.e., when the monitoring performances are poor) only a quite large scrap fraction (e.g., $\gamma > 0.2$ in this case study) motivates the use of in-situ defect detection.

In contrast, the machinery and aerospace case studies (Fig. 6 and Fig. 7) demonstrates that the availability of an in-situ monitoring tool was economically convenient even in the presence of quite low scrap fractions. This is mainly motivated by the longer duration of the LPBF process and by the higher material costs. For example, in the presence of good in-situ monitoring performances ($\alpha = 0.005$ and $\beta = 0.03$), the minimum scrap fraction at which an in-situ monitoring tool was economically convenient was lower than 0.05 in both cases. However, in the presence of poor in-situ monitoring performances ($\alpha = 0.05$ and $\beta = 0.3$), it was slightly lower than 0.2 for the machinery component and slightly higher than 0.1 for the aerospace bracket.

Fig. 5 to Fig. 7 show that the location of the intersection between the confidence bands and the cost curves in the different scenarios could be used as a driver to evaluate the economic convenience of in-situ monitoring tools. A parametric analysis of the location of this intersection as a function of the scrap fraction and the in-situ monitoring performances is depicted in Fig. 8.

Fig. 8 shows the minimum scrap fraction at which an in-situ monitoring tool was economically convenient in the *monitoring* scenario (Fig. 8, left panels) and the *monitoring & diagnosis* scenario (Fig. 8, right panels) for the dental prostheses (Fig. 8, top panels), the machinery component (Fig. 8, central panels), and the aerospace bracket (Fig. 8, bottom panels). The in-situ diagnosis analysis modifies the slope of the model in such a way that Type II error was most critical in influencing the minimum scrap fraction for

convenient use of in-situ monitoring tools (Fig. 8). Indeed, the diagnosis step was specifically aimed at identifying false alarms and avoiding undesired suppressions of non-defective parts. This mitigates the impact of Type I errors, but it introduces additional costs proportional to the overall time spent to carry out the diagnosis analysis during the LPBF process.

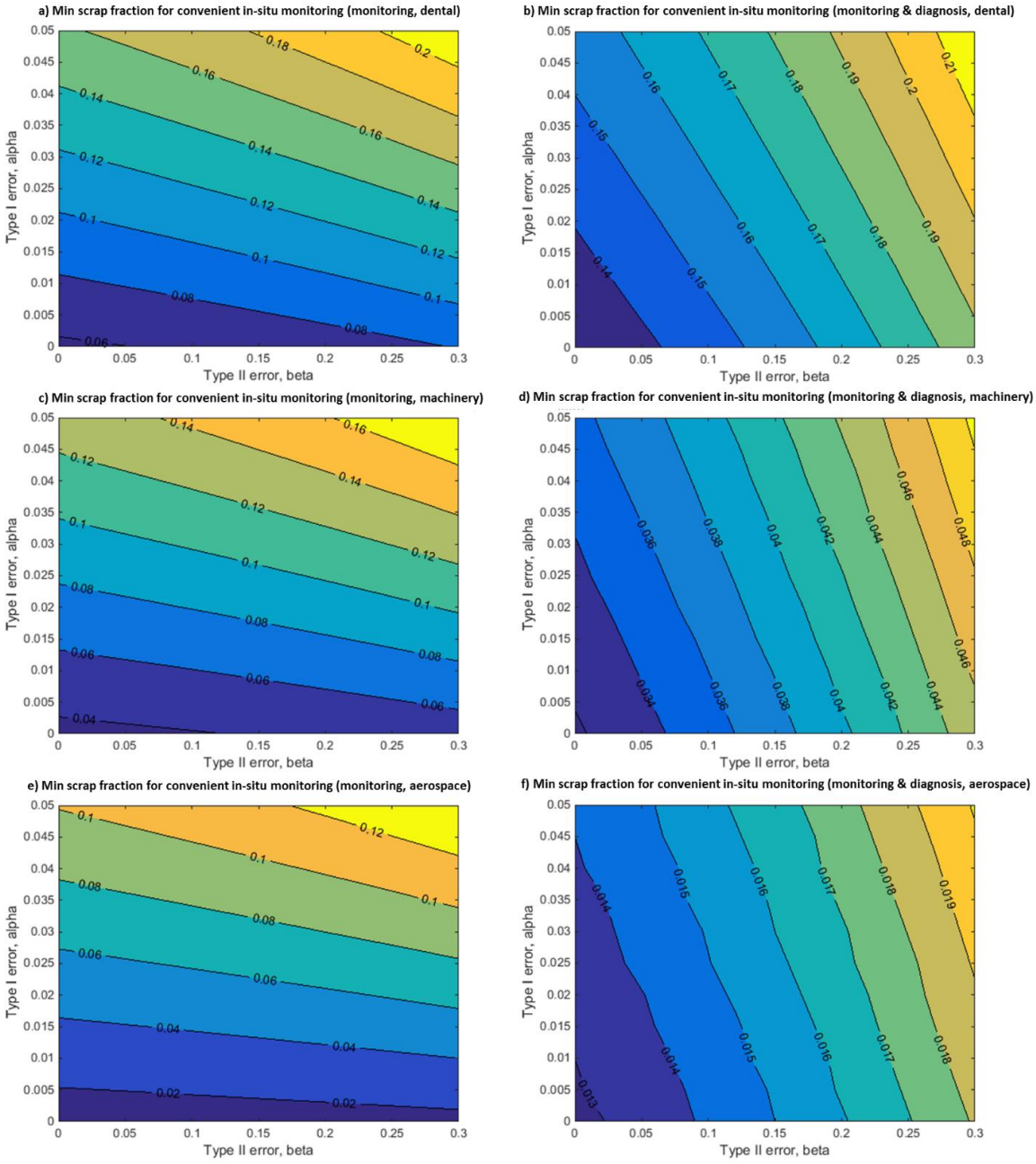


Fig. 8 – Minimum scrap fraction for convenient use of in-situ monitoring in the dental prostheses (top panels), machinery component (central panels), and aerospace bracket (bottom panels) case studies; left panels show the results for the *monitoring* scenario and right panels show results for the *monitoring & diagnosis* scenario

Fig. 8 (top panels) shows that, in a relatively low cost case study like the dental prostheses one, the additional diagnosis capability may be not economically convenient, because the associated extra-cost may overwhelm the cost imposed by interrupted processes as a consequence of false alarms. In contrast, a completely different effect was observed in the other two case studies. Indeed, Fig. 8 (central and bottom panels) shows that carrying out a diagnosis analysis may have considerably improved the economic sustainability of in-situ monitoring during the production of the machinery component and the aerospace bracket. For example, the availability of a diagnosis step made in-situ monitoring economically viable at quite low scrap fractions (i.e., $\gamma < 0.05$ in the machinery case study and $\gamma < 0.02$ in the aerospace case study), under the previously mentioned assumptions. Indeed, the extra diagnosis cost was negligible compared to the considerable cost reduction allowed by avoiding undesired part suppressions caused by false alarms. Thus, the longer the LPBF process was and the higher the net cost for producing a part was, the lower the minimum scrap fraction needed to justify the use of in-situ monitoring tools was. According to the assumptions stated in Section 3, the results shown in Fig. 8 refer to a fully reliable diagnosis. In the presence of misclassifications of false and actual alarms during the diagnosis step, the expected results are intermediate between the ones achieved in the *monitoring* scenarios and the ones achieved in the *monitoring & diagnosis* scenario.

### *4.2 Extra equipment costs*

All the results discussed above relied on the assumption that the cost of the in-situ monitoring equipment was embedded into the LPBF system cost. However, if this equipment was provided by the system developer at an extra cost, the proposed model allows one to determine the payback on the initial investment thanks to in-situ defect detection capabilities. For example, we estimated that the extra cost for the monitoring equipment was equal to either 50 k€ or 150 k€, which corresponds to an increase of $C_{LPBFsys}$ in the *monitoring* scenario from 28 €/h to 30.15 €/h and 34.65 €/h, respectively, whereas $C_{LPBFsys}$ in the *as-is* scenario did not change. Fig. 9 compares the part cost with and without in-situ monitoring capabilities at different extra costs for the monitoring equipment in the three different case studies. For sake of simplicity, the in-situ defect detection performances were set to $\alpha = 0.005$ and $\beta = 0.03$ (i.e., the best-case scenario).

Fig. 9a shows that for the production of relatively low cost and simple parts like the dental prostheses, increasing the hourly LPBF system cost made the in-situ monitoring functionality economically convenient when scrap fractions are larger than expected (i.e., $\gamma > 0.2$). However, Fig. 9b and Fig. 9c show that a payback of a larger initial investment can be achieved at scrap fractions in the range $\gamma = 0.15 - 0.4$ in the presence of more expensive products characterized by long duration LPBF processes. For example, in the machinery component case study, an extra cost of 50 k€ made in-situ monitoring economically viable at about $\gamma = 0.18$, and an extra cost of 150 k€ made it viable at about $\gamma = 0.4$. An analogous result was achieved in the aerospace bracket case study.

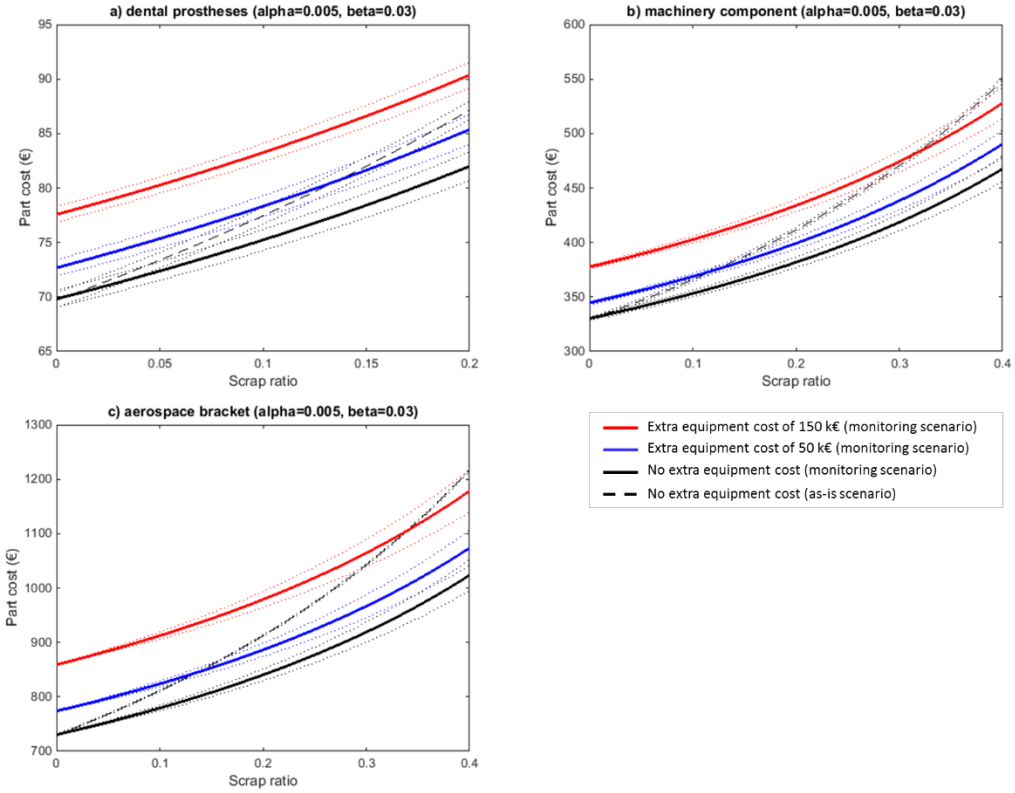


Fig. 9 – Comparison of the part cost curve in the as-is scenario and the monitoring scenario at different extra costs with 95% Bonferroni's confidence intervals (dotted lines) as a function of $\gamma$: a) dental prostheses, b) machinery component, and c) aerospace bracket

### *4.3 The make-or-buy option*

This sub-section investigates the economic benefits of in-situ monitoring tools from an additional perspective, i.e., not only in terms of overall cost reduction, but also in terms of increased production capacity. Since scrap reduction and early defective process interruption are enabled by in-situ monitoring

capabilities, a given target number of parts can be produced in a shorter time. This allows the company to produce more parts internally, reducing the need to externalize a portion of the production.

In AM series production, companies usually have to face the *make-or-buy* trade-off, i.e., the trade-off between internal and external production. Covering the entire AM production with in-house systems may be not feasible, and hence a portion of the production is externalized to AM service providers, with higher costs. However, an increased production capacity allow them to reduce the need for buying parts outside, with economic advantages that sum to cost savings discussed in previous sections of the paper.

For example, when $\gamma = 0.1$ in the dental prostheses case study, the average time to fabricate a defect-free part was $T_{proc} = 0.97\ h$ in the *as-is* scenario and $T_{proc} = 0.92\ h$ in the *monitoring* scenario (with $\alpha = 0.005$ and $\beta = 0.03$). Considering an LPBF system load factor of 55%, these two estimates led to a yearly production of 4585 parts in the *as-is* scenario and 4821 parts in the *monitoring* scenario, i.e., a 5% increase in productivity due to in-situ monitoring capabilities. One way to quantify the benefit of such higher productivity in the part cost analysis consists of introducing the make-or-buy option. Assume that the production capacity of the company is saturated in the *as-is* scenario: this means that any additional production needs to be externalized (i.e., "buy" choice). If we let $n$ be the number of parts actually produced and $N$ be the maximum number of parts that could be produced, we can than exploit in-situ monitoring capabilities. It is possible to introduce the make-or-buy option into the actual cost of a part as follows:

$$C_{actual} = \left(\frac{n}{N}\right) C_{make} + \left(\frac{N-n}{N}\right) C_{buy} \quad (€/\text{part}) \tag{19}$$

where $C_{make}$ is the cost for the internal production of one part (it coincides with the part cost, $C_{part}$, previously defined for the different scenarios) and $C_{buy}$ is then the net price of one part bought from an external company. By replacing $C_{part}$ with $C_{actual}$ in our cost model, it was possible to compare different scenarios by setting the target productivity at the highest level (i.e., the one offered by in-situ monitoring capabilities) and assessing the "buy" option in the *as-is* scenario to account for extra production. In the previous example, $n = 4585$ and $N = 4821$ in the *as-is* scenario, thus the $C_{actual}$ estimation was augmented

by the $C_{buy}$ term with a relative weight of 0.049. In the *monitoring* scenario, instead, $n = N$, thus only the $C_{make}$ term was considered.

If $C_{buy} = C_{make}$, the actual part cost would not be affected by the partial externalization of the production. However, $C_{buy}$ was expected to be larger than $C_{make}$ because of mark-up costs. The larger the gap between $C_{buy}$ and $C_{make}$ was, the higher the expected economic benefit of using in-situ monitoring methods was. Table 5 shows some examples of how the "buy" choice for extra production affects the comparison between different scenarios for different values of the $C_{buy}/C_{make}$ ratio. In Table 8, the minimum scrap fraction for convenient use of in-situ monitoring (*monitoring* scenario) is shown, based on the following monitoring performances: $\alpha = 0.005$ and $\beta = 0.03$. By taking into account the make-or-buy option for the gap in production capacity between the *as-is* and the *monitoring* scenario, the economic advantage provided by the in-situ monitoring capability increased as the $C_{buy}/C_{make}$ ratio increased. For example, the scrap fraction for a sustainable use of in-situ monitoring toolkits reduced from $\gamma > 0.4$ to $\gamma = 0.16$ when $C_{buy} = 2C_{make}$ at an extra equipment cost of 150 k€ in the dental prostheses case study, from $\gamma = 0.39$ to $\gamma = 0.19$ in the machinery component case study, and from $\gamma > 0.4$ to $\gamma = 0.2$ in the aerospace bracket case study. Instead, if the extra equipment costed 50 k€ in all of the case studies, the scrap fraction for a sustainable use of in-situ monitoring was $\gamma = 0.08$ when $C_{buy} = 2C_{make}$.

Table 5 – Min scrap fractions for convenient use of in-situ monitoring for different $C_{buy}/C_{make}$ ratios and extra equipment costs

| $C_{buy}/C_{make}$ | Extra equipment cost (k€) | Min scrap fraction for convenient use of in-situ monitoring | | |
|---|---|---|---|---|
| | | Dental prostheses | Machinery component | Aerospace bracket |
| 1 | 0 | 0.06 | 0.04 | 0.02 |
| | 50 | 0.21 | 0.18 | 0.18 |
| | 150 | >0.4 | 0.39 | >0.4 |
| 1.5 | 0 | 0.05 | 0.04 | 0.02 |
| | 50 | 0.11 | 0.10 | 0.10 |
| | 150 | 0.23 | 0.27 | 0.28 |
| 2 | 0 | 0.03 | 0.04 | 0.02 |
| | 50 | 0.08 | 0.08 | 0.08 |
| | 150 | 0.16 | 0.19 | 0.20 |

Fig. 9 and Table 5 show that the proposed cost model may be used to drive investment decisions where process monitoring systems represent optional equipment that comes at an extra cost. Such decisions depend

not only on the nature of the product, but also on the expected scrap fraction of the process, the make-or-buy trade-off, and the performances of the monitoring system itself.

## 5. VALIDATION

The goal of this analysis consists of validating the suitability of the proposed cost model to estimate the cost savings when in-situ monitoring toolkits are used to anticipate the detection of defective parts. To this aim, an experimental study was carried out in collaboration with one of the largest AM service bureaus in Europe, involving the production of complex shapes by means of an LPBF system equipped with a commercial in-situ monitoring tool. Some unrecoverable defects occurred in a subset of the produced parts, and these defects were properly detected by the in-situ monitoring tool. This allowed us to exploit this experimentation to compare the cost estimates in the *as-is* and *monitoring* scenarios obtained via our proposed cost model against the cost estimates in the same scenarios provided by the AM service bureau. Thus, the rationale behind the presented validation analysis consists of assessing the goodness of our model estimates with respect to a benchmark experimentation where real defective parts were produced and off-the-shelf monitoring tools were used.

### *5.1 Experimentation*

The experimentation consists of one Ti6Al4V LPBF build including nine copies of a tailor-made test shape composed by various critical features like large overhang areas, thin walls and lattice structures. A top view of the build is shown in Fig. 10. Three copies of the same part, labelled as 1A, 1B and 1C, were produced with the major axis parallel to the baseplate. Three more copies, labelled as 2A, 2B and 2C, were produced with the major axis parallel to the baseplate but placed upside-down with respect to the previous three copies. The remaining three copies, labelled as 3A, 3B and 3C, were placed with their major axis at a 45° angle from the baseplate.

Two copies, namely 1A and 1B, exhibited a warping of overhanging features that led to a detachment from supports, with consequent severe geometrical distortions in the as-built geometry that could not be recovered in post-process phases. The in-situ monitoring tool installed into the LPBF consists of a near infrared camera that acquires low speed videos during the production of each layer. In-situ gathered video

image streams are processed in real-time to generate layerwise heat maps that could be used to identify the presence of either cold or hot spots, i.e., areas of the build where a lack of energy density or an excessive heat accumulation occurred, respectively. Such in-situ monitoring tool signaled an anomalous hot spot in correspondence of the layers where the detachment from the supports in copies 1A and 1B actually occurred. The process was not stopped, but the post-process visual inspections and contactless geometry reconstructions confirmed the defective nature of copies 1A and 1B, whereas other copies were judged in-control.

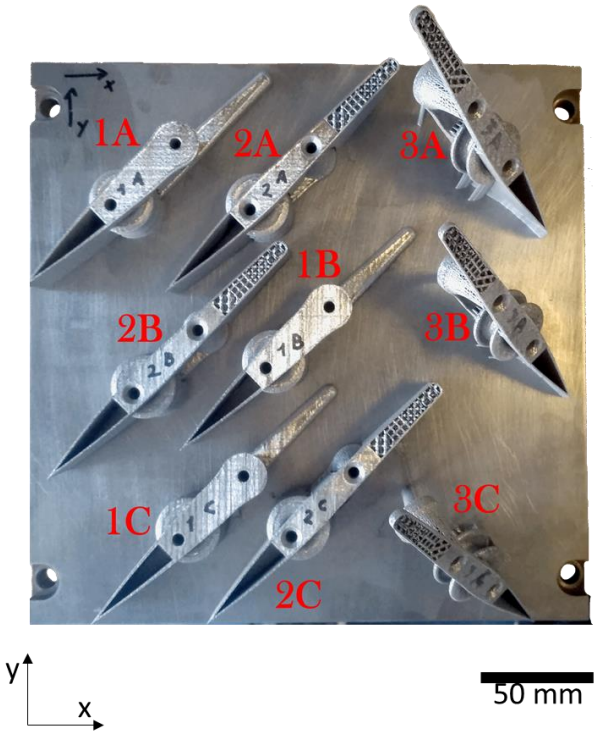


Fig. 10 – Top view of the LPBF build used for model validation, including nine copies of the tailor-made complex geometry

The model inputs to test our proposed cost model are summarized in Table 6. Various inputs were measured during the experimentation, including the baseplate area, the area of the interface between the part and the baseplate, the total duration of the LPBF process together with the duration of different process phases. Some inputs were provided directly by the AM service bureau where the experimentation was carried out (some of them can not be reported for privacy reasons). The scrap fraction was set to $\gamma = 0.22$, as two parts out of nine in the build presented defects at the end of the process. The completion rate, $CR = 0.27$, was measured as the fraction of the copies 1A and 1B produced before the detachment from supports was

signaled by the in-situ monitoring tool. Regarding the estimate of Type I and Type II errors, the following approach was applied. First, based on previous LPBF productions on the same machine with the in-situ monitoring system installed, a preliminary estimate of ranges for these two errors was drawn, i.e., false alarm rates were observed in the range $\alpha \in [1 - 5]\%$ and missed detection rates were observed in the range $\beta \in [10 - 20]\%$. Monte Carlo simulations were then carried out based on Type I and Type II error gathered as random numbers assuming a uniform distribution of both errors in given ranges.

Table 6 – Summary of model inputs and their source for the model validation experimental study (additional input values provided by the AM service bureau not reported for privacy reasons)

| Parameter | Values | Source of information |
|---|---|---|
| $P_{price}$ (€/kg) | 200 | AM service bureau |
| $V$ ($m^3$) | $1.84*10^{-5}$ | CAD model |
| $\rho$ ($kg/m^3$) | 4430 | Material specification for Ti6Al4V |
| $w$ | 0.01 | AM service bureau |
| $T_{buildprep}$ (h) | 0.1 | AM service bureau |
| $n_p$ | 9 | Experimental plan |
| $A_{baseplate}$ ($m^2$) | 0.0625 | Direct measurement |
| $A_{part}$ ($m^2$) | $1*10^{-5}$ | Direct measurement |
| $\alpha$ | 1% - 5% | Previous experimental results at AM service bureau |
| $\beta$ | 10% - 20% | Previous experimental results at AM service bureau |
| $\gamma$ | 0.22 | Two defective copies out of nine in the build |
| $CR$ | 0.27 | In-situ monitoring tool signal |
| $T_{setup}$ (h) | 1.5 | Real duration (measured) |
| $T_{build}$ (h) | 16.1 | Real duration (measured) |
| $T_{removal}$ (h) | 0.5 | Real duration (measured) |
| $T_{inspection}$ (h) | 0.5 | Real duration (measured) |

### *5.2 Discussion*

The cost estimates were generated in two scenarios. The benchmark cost estimate in the *as-is* scenario refers to the cost for the production of the entire build, without interruptions, followed by the production of a second build including only the two defective copies placed with a different orientation (i.e., the same orientation of copies 2A, 2B and 2C that were printed without defects) to avoid the re-occurrence of geometrical distortions. In the *monitoring scenario*, instead, the production of copies 1A and 1B was interrupted once the defect was signaled by the in-situ monitoring tool, and only the remaining copies were produced without interruptions. Also in this case one additional build was need to finally produce nine parts without defects. The difference between the estimated costs in these two scenarios represents the estimated cost savings provided by the availability of an in-situ process monitoring method. The benchmark cost

estimate in both the scenarios was provided by the AM service bureau based on internal cost estimation policies. The results are summarized in Table 7.

Table 7 – Cost estimates and benchmark costs estimates in the model validation experimental study (standard deviation is reported in bracket for the cost estimate based on proposed model in the monitoring scenario)

| | Cost estimate (€/part) | | Average saving thanks to in-situ monitoring |
|---|---|---|---|
| | As-is scenario | Monitoring scenario | |
| Estimate based on proposed model | 212.74 | 192.99 (1.32) | 9.28 % |
| Benchmark cost from AM service bureau | 234.67 | 205.93 | 9.88 % |

Table 7 shows that the proposed model yields an average saving thanks to the availability of in-situ defect detection capabilities of about 9.28%, whereas the benchmark estimate is about 9.88%. The two estimates are of the same order of magnitude, with a slight under-estimate of costs in both the as-is and monitoring scenarios. Such under-estimate is mainly caused by the fact that the benchmark cost estimate from the AM service bureau relies on a forfeit hourly-cost definition for the LPBF process that is slightly higher than the one based on the cost model presented in this study. However, the different between the two cost estimates is lower than 10%. The results in Table 7 indicate that the proposed cost model is suitable to generate reasonable estimates of the economic viability of in-situ monitoring tools. It is also suitable to generate robust estimates, thanks to the capability of evaluating the uncertainty related to Type I and Type II errors via Monte Carlo simulations. Further experimentations are foreseen to further validate the proposed cost model in different AM applications.

## 6. CONCLUSION

Thanks to continuous technological developments, metal AM systems have become suitable not only for rapid prototyping applications, but also for final product manufacturing in various industrial sectors. Because of this, the integration of AM processes into existing or new production environments requires reliable economic models to support trade-off analysis and investment decisions. Indeed, increasing attention has been devoted to the development of cost models in the field of metal AM applications. The mainstream objective in the reference literature consists of evaluating the economic convenience of metal AM systems compared to traditional approaches. However, there is still a lack of economic analysis that takes into account the defectiveness of the production process and the suitability of methods for scrap and material waste

reduction. This study presented a generalized cost model formulation to determine the economic impact of defects in metal PBF processes and the economic convenience of in-situ monitoring solutions. The main output of the model consists of parametric maps that depend on the Type I (false alarms, alpha) and Type II (false negatives, beta) errors. The goodness and appropriateness of our model assumptions, together with the effect of those assumptions on the parametric maps generated by the model as a function of Type I and Type II errors, were first verified by means of interviews with representatives of AM companies. An experimental study was then carried out in collaboration with one of the largest AM service bureau in Europe to validate the proposed cost model with respect to a benchmark reference. Three additional real case studies were presented to test and demonstrate the suitability of the proposed methodology in the presence of real industrial processes, with real data as model inputs based on the manufacturing of those same parts via LPBF and on literature data. They allowed us to show that the model can be used not only to assess the relevance of in-situ monitoring methods for advanced metal AM systems, but also to assess the performance specifications, in terms of target Type I and Type II errors, that make in-situ monitoring actually convenient in specific applications. Complete details and model inputs in real case studies were provided to allow the replication of the presented results, but the flexibility and generality of the model allows extending the analysis to the production of any other metal part via LPBF. Generally speaking, the proposed model relies on clearly stated assumptions and it lacks implicit or hidden function, which makes it easily applicable to any other case study in AM. From a managerial implication viewpoint, the results of the study allow identifying three categories of products in AM, namely low-, medium-, and high-value-added products. For the first category, an in-situ monitoring tool results to be not economically convenient (apart from contingent situations where quite high scrap fractions are met), because the detrimental effect of false alarms counterbalances the potential benefits of in-line defect detection. For the second category, the economical convenience of this kind of tools is likely, but it depends on the performances of the monitoring tool in terms of false alarms and false negatives. If the monitoring tool is poorly reliable, it may be not economically convenient also in this case. In this framework, the proposed model allows one to determine whether and when the use of an in-situ monitoring tool is viable. As an example, an experimental campaign can be designed to characterize the performances of the monitoring algorithm and decide whether its performances need to be tuned. In the third case, i.e., high-value-added products, the availability of an in-situ monitoring

tool is convenient even in the presence of non-optimal fault detection performances, because high manufacturing and material costs to produce one part make the production of scraps quite critical.

In the present study, part suppression during the build was the only action considered as a consequence of an in-situ defect detection. This is representative of state-of-the-art LPBF systems where proprietary controllers do not include feedback control loops based on in-situ gathered data. However, novel integrated control solutions can be envisaged for next generation systems, which may allow one to repair the defect while the part has been built and/or adapt the process parameters to avoid defect propagation to following layers. Few seminal studies have been devoted to this topic so far (Mireles *et al*., 2015b, Yasa *et al*., 2011), but further research efforts in this field are foreseen in the future. The proposed model may be extended and adapted to include such in-situ defect handling and control capabilities.

## REFERENCES


Alexander, P., Allen, S. and Dutta, D. (1998), Part orientation and build cost determination in layered manufacturing, Computer-Aided Design, 30(5), 343-356.

Ashby, M. (1999), Material selection in mechanical design, 3rd edition, Oxford, Elsevier Butterworth-Heinemann

Atzeni, E., Salmi, A. (2012), Economics of additive manufacturing for end-usable metal parts, The International Journal of Advanced Manufacturing Technology, 62(9-12), 1147

Baumers, M., Dickens, P., Tuck, C., & Hague, R. (2016). The cost of additive manufacturing: machine productivity, economies of scale and technology-push. Technological forecasting and social change, 102, 193-201.

Bayle, F., & Doubenskaia, M. (2008). Selective laser melting process monitoring with high speed infra-red camera and pyrometer. In Fundamentals of Laser Assisted Micro-and Nanotechnologies (pp. 698505-698505). International Society for Optics and Photonics.

Berger, R. (2013), Additive manufacturing: a game changer for the manufacturing industry. Roland Berger Strategy Consultants GmbH, Munich.

Berumen, S., Bechmann, F., Lindner, S., Kruth, J. P., & Craeghs, T. (2010). Quality control of laser-and powder bed-based Additive Manufacturing (AM) technologies. Physics procedia, 5, 617-622.

Caltanissetta F., Grasso M., Petrò S., Colosimo, B. M. (2018). Characterization of In-Situ Measurements based on Layerwise Imaging in Laser Powder Bed Fusion, Additive Manufacturing, 24, 183-199

Chivel, Y. (2013). Optical in-process temperature monitoring of selective laser melting. Physics Procedia, 41, 904-910.

Clijsters, S., Craeghs, T., Buls, S., Kempen, K., & Kruth, J. P. (2014). In situ quality control of the selective laser melting process using a high-speed, real-time melt pool monitoring system. The International Journal of Advanced Manufacturing Technology, 75(5-8), 1089-1101.

Craeghs, T., Bechmann, F., Berumen, S., & Kruth, J. P. (2010). Feedback control of Layerwise Laser Melting using optical sensors. Physics Procedia, 5, 505-514.

Craeghs, T., Clijsters, S., Kruth, J. P., Bechmann, F., & Ebert, M. C. (2012). Detection of process failures in layerwise laser melting with optical process monitoring. Physics Procedia, 39, 753-759.

Craeghs, T., Clijsters, S., Yasa, E., Bechmann, F., Berumen, S., & Kruth, J. P. (2011). Determination of geometrical factors in Layerwise Laser Melting using optical process monitoring. Optics and Lasers in Engineering, 49(12), 1440-1446.

Dinwiddie, R. B., Dehoff, R. R., Lloyd, P. D., Lowe, L. E., & Ulrich, J. B. (2013, May). Thermographic in-situ process monitoring of the electron-beam melting technology used in additive manufacturing. In SPIE Defense, Security, and Sensing (pp. 87050K-87050K). International Society for Optics and Photonics.

Doubenskaia, M. A., Zhirnov, I. V., Teleshevskiy, V. I., Bertrand, P., & Smurov, I. Y. (2015). Determination of true temperature in selective laser melting of metal powder using infrared camera. In Materials Science Forum (Vol. 834, pp. 93-102). Trans Tech Publications.

Doubenskaia, M., Pavlov, M., Grigoriev, S., Tikhonova, E., & Smurov, I. (2012). Comprehensive optical monitoring of selective laser melting. Journal of Laser Micro Nanoengineering, 7(3), 236-243.

Dunbar, A. J. (2016). Analysis of the Laser Powder Bed Fusion Additive Manufacturing Process Through Experimental Measurement and Finite Element Modeling (Doctoral dissertation, The Pennsylvania State University).

EOS web site (last access: 06/02/2017), Medical (Dental): BEGO USA - Patient specific restorations made of a high-performance alloy, https://www.eos.info/press/customer_case_studies/bego

Everton, S. K., Hirsch, M., Stravroulakis, P., Leach, R. K., & Clare, A. T. (2016). Review of in-situ process monitoring and in-situ metrology for metal additive manufacturing. Materials & Design, 95, 431-445.

Foster, B. K., Reutzel, E. W., Nassar, A. R., Hall, B. T., Brown, S. W., & Dickman, C. J. (2015) Optical, layerwise monitoring of powder bed fusion. In Solid Free. Fabr. Symp. Proc, 295-307.

Gibson, I., Rosen, D. W., Stucker, B. (2010). Additive manufacturing technologies. New York: Springer.

Gong, X., Cheng, B., Price, S., & Chou, K. (2013). Powder-bed electron-beam-melting additive manufacturing: powder characterization, process simulation and metrology. In Proceedings of the ASME District F Early Career Technical Conference, 59-66.

Grasso, M., Colosimo, B.M. (2019), A Statistical Learning Method for Image-based Monitoring of the Plume Signature in Laser Powder Bed Fusion, Robotics and Computer-Integrated Manufacturing, 57, 103-115

Grasso M., Colosimo B.M., (2017), Process Defects and In-situ Monitoring Methods in Metal Powder Bed Fusion: a Review, Measurement Science and Technology, 28(4), 1-25, DOI: 10.1088/1361-6501/aa5c4f

Grasso, M., Demir, A.G., Previtali, B., Colosimo, B.M. (2018), In-situ Monitoring of Selective Laser Melting of Zinc Powder via Infrared Imaging of the Process Plume, Robotics and Computer-Integrated Manufacturing, 49, 229-239. https://doi.org/10.1016/j.rcim.2017.07.001

Grasso, M., Laguzza, V., Semeraro, Q., & Colosimo, B. M. (2016). In-process Monitoring of Selective Laser Melting: Spatial Detection of Defects via Image Data Analysis. Journal of Manufacturing Science and Engineering, 139(5), 051001-1 – 051001-16.

Hart, J. (2015), Cost and value analysis of AM, Additive Manufacturing Summer School Report 2015, MIT

Hopkinson, N., Dickens, P.M. (2003), Analysis of rapid manufacturing using layer manufacturing processes for production, proceedings of the Institute of Mechanical Engineers, Part C: Journal of Mechanical Engineering Science, 217 (C1), 31-39.

Huang, R., Riddle, M. E., Graziano, D., Das, S., Nimbalkar, S., Cresko, J., & Masanet, E. (2017). Environmental and economic implications of distributed additive manufacturing: The case of injection mold tooling. Journal of Industrial Ecology, 21(S1).

Islam, M., Purtonen, T., Piili, H., Salminen, A., & Nyrhilä, O. (2013). Temperature profile and imaging analysis of laser additive manufacturing of stainless steel. Physics Procedia, 41, 835-842.

Kanko, J. A., Sibley, A. P., & Fraser, J. M. (2016). In situ morphology-based defect detection of selective laser melting through inline coherent imaging. Journal of Materials Processing Technology, 231, 488-500.

Kleszczynski, S., zur Jacobsmühlen, J., Reinarz, B., Sehrt, J. T., Witt, G., & Merhof, D. (2014). Improving process stability of laser beam melting systems. In Proceedings of the Frauenhofer Direct Digital Manufacturing Conference.

Kleszczynski, S., zur Jacobsmühlen, J., Sehrt, J. T., & Witt, G. (2012). Error detection in laser beam melting systems by high resolution imaging. In Proceedings of the Solid Freeform Fabrication Symposium.

Krauss, H., Eschey, C., & Zaeh, M. (2012). Thermography for monitoring the selective laser melting process. In Proceedings of the Solid Freeform Fabrication Symposium.

Krauss, H., Zeugner, T., & Zaeh, M. F. (2014). Layerwise monitoring of the selective laser melting process by thermography. Physics Procedia, 56, 64-71.

Kruth, J. P., Mercelis, P., Van Vaerenbergh, J., & Craeghs, T. (2007). Feedback control of selective laser melting. In Proceedings of the 3rd international conference on advanced research in virtual and rapid prototyping (pp. 521-527).

Land, W. S., Zhang, B., Ziegert, J., & Davies, A. (2015). In-situ metrology system for laser powder bed fusion additive process. Procedia Manufacturing, 1, 393-403.

Lane, B., Moylan, S., Whitenton, E. P., & Ma, L. (2015). Thermographic Measurements of the Commercial Laser Powder Bed Fusion Process at NIST. In Proc. Solid Free. Fabr. Symp (Vol. 575).

Langefeld, B. (2013). Additive manufacturing–a game changer for the manufacturing industry? Roland Berger Strategy Consultants, München.

Laureijs, R. E., Roca, J. B., Narra, S. P., Montgomery, C., Beuth, J. L., & Fuchs, E. R. (2017). Metal Additive Manufacturing: Cost Competitive Beyond Low Volumes. Journal of Manufacturing Science and Engineering, 139(8), 081010.

Lindemann, C., Jahnke, U., Moi, M., Koch, R. (2012), Analyzing product lifecycle costs for a better understanding of cost drivers in Additive Manufacturing, proceedings of the Solid Freeform Fabrication Symposium, 177-188

Mani, M., Lane, B., Donmez, A., Feng, S., Moylan, S., & Fesperman, R. (2015). Measurement science needs for real-time control of additive manufacturing powder bed fusion processes. National Institute of Standards and Technology, Gaithersburg, MD, NIST Interagency/Internal Report (NISTIR), 8036.

Mellor, S., Hao, L., & Zhang, D. (2014). Additive manufacturing: A framework for implementation. International Journal of Production Economics, 149, 194-201.

Mireles, J., Ridwan, S., Morton, P. A., Hinojos, A., & Wicker, R. B. (2015b). Analysis and correction of defects within parts fabricated using powder bed fusion technology. Surface Topography: Metrology and Properties, 3(3), 034002.

Mireles, J., Terrazas, C., Gaytan, S. M., Roberson, D. A., & Wicker, R. B. (2015b). Closed-loop automatic feedback control in electron beam melting. The International Journal of Advanced Manufacturing Technology, 78(5-8), 1193-1199.

Montgomery, D. C. (2009). Statistical quality control (Vol. 7). New York: Wiley.

Neef, A., Seyda, V., Herzog, D., Emmelmann, C., Schönleber, M., & Kogel-Hollacher, M. (2014). Low coherence interferometry in selective laser melting. Physics Procedia, 56, 82-89.

Pavlov, M., Doubenskaia, M., & Smurov, I. (2010). Pyrometric analysis of thermal processes in SLM technology. Physics Procedia, 5, 523-531.

Price, S., Cooper, K., & Chou, K. (2012). Evaluations of temperature measurements by near-infrared thermography in powder-based electron-beam additive manufacturing. In Proceedings of the Solid Freeform Fabrication Symposium (pp. 761-773). University of Texas, Austin, TX.

Reinarz, B., Witt, G. (2012), Process monitoring in the laser beam melting process – Reduction of process breakdowns and defective parts, Material Science & Technology Conference, 2012

Repossini G., Laguzza V., Grasso M., Colosimo B.M., (2017), *On the use of spatter signature for in-situ monitoring of Laser Powder Bed Fusion*, Additive Manufacturing, 16, 35-48. https://doi.org/10.1016 /j.addma.2017.05.004.

Rickenbacher, L., Spierings, A., Wegener, K. (2013), An integrated cost-model for selective laser melting (SLM), Rapid Prototyping Journal, 19(3), 208 – 214

Ridwan, S., Mireles, J., Gaytan, S. M., Espalin, D., & Wicker, R. B. (2014). Automatic layerwise acquisition of thermal and geometric data of the electron beam melting process using infrared thermography. In Proc. Int. Symp. Solid Freeform Fabrication (Vol. 343).

Rieder, H., Dillhöfer, A., Spies, M., Bamberg, J., & Hess, T. (2014). Online monitoring of additive manufacturing processes using ultrasound. In Proceedings of the 11th European Conference on Non-Destructive Testing, October (pp. 6-10).

Rodriguez, E., Medina, F., Espalin, D., Terrazas, C., Muse, D., Henry, C., ... & Wicker, R. B. (2012). Integration of a thermal imaging feedback control system in electron beam melting. In Proceedings of the Solid Freeform Fabrication Symposium.

Rodriguez, E., Mireles, J., Terrazas, C. A., Espalin, D., Perez, M. A., & Wicker, R. B. (2015). Approximation of absolute surface temperature measurements of powder bed fusion additive manufacturing technology using in situ infrared thermography. Additive Manufacturing, 5, 31-39.

Ruffo, M. and Hague, R. (2007), Cost estimation for rapid manufacturing – simultaneous production of mixed components using laser sintering, Proceedings of the Institution of Mechanical Engineers, Part B: Journal of Engineering Manufacture, 221(11), 1585-1591.

Ruffo, M., Tuck, C. and Hague, R. (2006), Cost estimation for rapid manufacturing – laser sintering production for low to medium volumes, Proceedings of the Institution of Mechanical Engineers, Part B: Journal of Engineering Manufacture, 220(9), 1417-1427.

Sames, W. J., List, F. A., Pannala, S., Dehoff, R. R., & Babu, S. S. (2016). The metallurgy and processing science of metal additive manufacturing. International Materials Reviews, 1-46.

Schilp, J., Seidel, C., Krauss, H., & Weirather, J. (2014). Investigations on temperature fields during laser beam melting by means of process monitoring and multiscale process modelling. Advances in Mechanical Engineering, 6, 217584.

Schwerdtfeger, J., Singer, R. F., & Körner, C. (2012). In situ flaw detection by IR-imaging during electron beam melting. Rapid Prototyping Journal, 18(4), 259-263.

Sharratt, B. M. (2015). Non-Destructive Techniques and Technologies for Qualification of Additive Manufactured Parts and Processes. A literature Review. Contract Report DRDC-RDDC-2015-C035, Victoria, BC.

Spears, T. G., & Gold, S. A. (2016). In-process sensing in selective laser melting (SLM) additive manufacturing. Integrating Materials and Manufacturing Innovation, 5(1), 1.

Tapia, G., & Elwany, A. (2014). A review on process monitoring and control in metal-based additive manufacturing. Journal of Manufacturing Science and Engineering, 136(6), 060801.

Thomas, D. S., Gilbert, S. W. (2014). Costs and cost effectiveness of additive manufacturing. NIST Special Publication, 1176, http://dx.doi.org/10.6028/NIST.SP.1176

Thomas-Seale, L. E. J., Kirkman-Brown, J. C., Attallah, M. M., Espino, D. M., & Shepherd, D. E. T. (2018). The barriers to the progression of additive manufacture: Perspectives from UK industry. International Journal of Production Economics, 198, 104-118.

Thombansen, U., Gatej, A., & Pereira, M. (2015). Process observation in fiber laser–based selective laser melting. Optical Engineering, 54(1), 011008-011008.

Tomlin, M., & Meyer, J. (2011). Topology optimization of an additive layer manufactured (ALM) aerospace part. In Proceeding of the 7th Altair CAE technology conference (pp. 1-9).

Van Gestel, C. (2015). Study of physical phenomena of selective laser melting towards increased productivity. PhD Dissertation, Ecole Polytechnique Federale De Lausanne

Wegner, A., & Witt, G. (2011). Process monitoring in laser sintering using thermal imaging. In SFF Symposium, Austin, Texas, USA (pp. 8-10).

Weller, C., Kleer, R., & Piller, F. T. (2015). Economic implications of 3D printing: Market structure models in light of additive manufacturing revisited. International Journal of Production Economics, 164, 43-56.

Wohlers, T. (2018). Wohlers Report 2018: 3D Printing and Additive Manufacturing State of the Industry: Annual Worldwide Progress Report. Wohlers Associates.

Yadroitsev, I., Krakhmalev, P., & Yadroitsava, I. (2014). Selective laser melting of Ti6Al4V alloy for biomedical applications: Temperature monitoring and microstructural evolution. Journal of Alloys and Compounds, 583, 404-409.

Yasa, E., Kruth, J. P., & Deckers, J. (2011). Manufacturing by combining selective laser melting and selective laser erosion/laser re-melting. CIRP Annals-Manufacturing Technology, 60(1), 263-266.

Yin, R. K. (2009). Case study research: Design and methods (applied social research methods). London and Singapore: Sage.

Zhang, B., Ziegert, J., Farahi, F., & Davies, A. (2016). In situ surface topography of laser powder bed fusion using fringe projection. Additive Manufacturing, 12, 100-107.

Zur Jacobsmühlen, J., Kleszczynski, S., Schneider, D., & Witt, G. (2013). High resolution imaging for inspection of laser beam melting systems. In 2013 IEEE International Instrumentation and Measurement Technology Conference (I2MTC) (pp. 707-712). IEEE.

Zur Jacobsmühlen, J., Kleszczynski, S., Witt, G., & Merhof, D. (2015). Elevated Region Area Measurement for Quantitative Analysis Of Laser Beam Melting Process Stability. In Instrum. Meas. Technol. Conf. I2MTC (pp. 707-712).

## Appendix A – Summary of in-situ monitoring tools for PBF processes

Table A1 – Summary of the literature and commercial systems devoted to in-situ monitoring in metal PBF processes.

| ***Scientific literature*** | | |
|---|---|---|
| **Monitoring setup** | **In-situ sensing** | **Literature** |
| Co-axial | Pyrometry | *Clijsters et al., 2014; Craeghs et al., 2010-2011; Berumen et al., 2010; Chivel, 2013; Doubenskaia et al., 2012; Pavlov et al., 2010; Thombansen et al., 2015* |
| | Imaging (visible to near infrared) | *Clijsters et al., 2014; Craeghs et al., 2010-2012; Berumen et al., 2010; Chivel, 2013; Doubenskaia et al., 2012; Kruth et al., 2007; Van Gestel, 2015; Yadroitsev et al., 2014* |
| | Interferometric imaging | *Kanko et al., 2016; Neef et al., 2014* |
| Off-axis | Pyrometry | *Bayle and Doubenskaia, 2008; Islam et al., 2013* |
| | Imaging (visible to near infrared) | *Zur Jacobsmühlen et al., 2013, 2015;Kleszczynski et al., 2012; Land et al., 2015; Zhang et al., 2016; Grasso et al., 2016; Foster et al., 2015; Repossini et al., 2017; Caltanissetta et al., 2018* |
| | Thermal imaging (near to long wavelength infrared) | *Doubenskaia et al., 2015; Gong et al., 2013; Price et al., 2012; Krauss et al., 2012, 2014; Lane et al., 2015; Bayle and Doubenskaia, 2008; Schilp et al., 2014; Ridwan et al., 2014; Schwerdtfeger et al., 2012; Mireles et al., 2015; Dinwiddie et al., 2013; Rodriguez et al., 2012, 2015; Wegner and Witt, 2011; Grasso et al., 2018; Grasso and Colosimo, 2019* |
| Other | | *Kleszczynski et al., 2014; Reinarz and Witt, 2012; Rieder et al., 2014; Dunbar, 2016* |
| ***Commercial systems*** | | |
| **Company** | **Toolkit** | **In-situ sensing** |
| Concept Laser | QM meltpool 3d | Co-axial photodiodes & cameras |
| | QM coating | Off-axis camera |
| EOS | EOSTATE meltpool | Co-axial and off-axial photodiodes |
| | EOSTATE Exposure OT | Off-axis camera |
| | EOSTATE Powderbed | Off-axis camera |
| SLM Solutions | Meltpool Monitoring System | Co-axial photodiodes |
| | Laser Power Monitoring | Actual emitted laser output measurement |
| | Layer control systems | Off-axis camera |
| Renishaw | | Co-axial photodiodes |
| Arcam | LayerQam | Off-axis camera |
| Aconity 3D | Extensive Process Monitoring | Co-axial photodiodes & cameras |
| Sigma Labs | PrintRite3D | Co-axial and off-axis photodiodes and cameras |

Table A1 shows that different sensing methods are available. Co-axial sensing configurations involve the installation of sensors (e.g., photodiodes or cameras) within the optical path of the laser to monitor the properties of the melt pool (the small region heated above melting temperature) which helps determine the quality and stability of the process. This kind of monitoring setup is only possible in LPBF. In contrast, off-axial sensing configurations involve the placement of sensors outside of the optical path of the energy source. They can be used to detect defects that originate along the scan path, geometrical errors of the slice, or irregularities in the powder bed recoating. A few other sensing solutions have been proposed, e.g., the use

of accelerometers on the recoater (Kleszczynski *et al.*, 2014, - Reinarz and Witt, 2012) and ultrasound sensors (Dunbar, 2016).

## Appendix B – Ethical statement

To the aim of verifying the goodness and appropriateness of our model assumptions and to validate its cost estimates with respect to industrial benchmarks, interviews with representatives of AM companies were carried out and an experimental validation study was performed together with one of the largest AM service bureau in Europe. These activities were carried out in compliance with the European General Data Protection Regulation GDPR (https://eur-lex.europa.eu/legal-content/EN) and with the Regulation for the Research Ethical Issues defined by the authors' affiliation institute.

In particular, the following approaches were followed:

- Informed consent. All the interviewed people and the persons involved in the research received a clear statement of what the research was about, what it involves, and what their contribution could be. Organizations' approval and express permission to get involved in the research were recorded before interviews and experimental activities.
- Anonymisation. All the interviewed people requested to remaining anonymous, therefore no information about individuals and their affiliations are reported in this paper; the full text of the paper was verified before each review step and the content was agreed with all the involved persons.
- Data protect. A specific agreement was recorded with all the individuals and entities involved in the research related to the use of data. Only data that were classified as "public" have been included in the present paper. All other data were kept as confidential and the authors committed to protect sensitive data avoiding any unauthorized use.